Soil Dynamics and Earthquake Engineering 100 (2017) 16–33

Contents lists available at ScienceDirect

Soil Dynamics and Earthquake Engineering

journal homepage: www.elsevier.com/locate/soildyn

Seismic demand and experimental evaluation of the nonstructural building curtain wall: A review

Baofeng Huang[a], Shiming Chen[b], Wensheng Lu[b,*], Khalid M. Mosalam[c]

[a] College of Civil Engineering, Nanjing Tech University, Nanjing, PR China
[b] Research Institute of Structural Engineering and Disaster Reduction, Tongji University, Shanghai, PR China
[c] Department of Civil & Environmental Engineering, University of California, Berkeley, CA, USA

ARTICLE INFO

Keywords:
Curtain wall
Acceleration demand
Drift demand
Fragility
Seismic performance
Shaking table
Testing protocol

ABSTRACT

This paper reviews the existing studies related to seismic demand and experimental investigation of the nonstructural building curtain wall (CW). Being treated as a nonstructural component, seismic performance of the building CW relates to its seismic demand parameters, i.e., acceleration and drift demands. In current code provisions, the acceleration demand consists of the floor acceleration amplification factor, component acceleration amplification factor, component importance factor, and component response modification factor, which are all based on or induced by the floor response and dynamic response of the CW itself. For the CW which is attached to the main structure, drift demand is an indication of the interstory drift ratio. The in-plane seismic drift mechanism of the framed glass CW was fully developed, and the corresponding static testing protocols were implemented in codes based on several past experimental studies. Shaking table testing of the CW was conducted as well, where the input motions need specific floor response analysis of the main structure. The relevant damage state definition and fragility curve development are important to represent the performance and damage level of the CW system. The philosophy of the performance-based earthquake engineering (PBEE) and its application to CW are elaborated, and possible challenges related to the seismic demand, experimental studies, and PBEE of the CW are addressed as well.

1. Introduction

Curtain wall (CW) indicates any building wall, of any material (e.g. stone, reinforced concrete, glass, metal, etc.), which carries no superimposed vertical loads, i.e., any 'nonbearing' wall. Building CW or façade provides the aesthetic, environmental, and structural functions to achieve the enclosure required for the safety, comfort and functionality of building occupants and contents. Precast reinforced concrete (RC), stone, and masonry are materials typically used in building facade. Due to the rapid development of manufacture and construction technologies, glass, steel, or natural stone panels are easily produced with lower cost than before, thus light and aesthetic façades are very popular in modern, especially tall and landmark, buildings. There are several terminologies used for the building façade, such as cladding, building envelope, and curtain wall. In this paper, however, curtain wall is used. Nowadays, compared to the traditional CW (e.g., masonry or stone CW), glass CW is light in mass, transparent, and relatively energy efficient. Therefore, glass CW became the most popular façade type.

In some countries (e.g., China), CW was architecturally conceived by the architect who is usually not involved in the structural design. Therefore, the load bearing or transfer profile of these CWs are not typically considered during the structural design. In practice, the construction industry usually conducted design, fabrication and installation of the CW in the building structure, with little or no consideration of structural analysis. Therefore, the structural performance of the CW would not be ensured. Nowadays, the CW design codes have been enforced where the CWs are designed by the CW designer company, the architect, or the structural engineer. The glass thickness, material, configuration, framing, and connections have to be designed for gravity and lateral wind/seismic loads. Furthermore, compared to the traditional structural elements, e.g., columns, slabs and girders, CW is relatively a novel subsystem in the modern building structural system, and the real earthquake damage observations are still rare. Although the seismic performance of CW system has become a greater concern to engineers due to the numerous CW failure cases in the past decades, seismic safety of the substantial amount of CWs cannot be verified by real earthquakes, even if they are carefully designed by qualified structural engineers. Study on the seismic performance of the CW system is scarcely reported in the literature. However, although CW is

* Corresponding author.

http://dx.doi.org/10.1016/j.soildyn.2017.05.025
Received 13 December 2016; Received in revised form 31 March 2017; Accepted 16 May 2017
Available online 23 May 2017

treated as a nonstructural component (NC), it should have the ability to transfer the inertia load to the main structure, and must be able to accommodate the story drift of the main building. Under the framework of performance-based earthquake engineering (PBEE), reducing the earthquake damage of the NCs, including the CW system, can decrease the cost due to earthquake losses considerably. Accordingly, reducing the earthquake damage to the CW system is a direct objective of the performance-based seismic design.

In this paper, code provisions on seismic demands (i.e., acceleration and drift demands) and seismic experimental methods, damage mechanisms, and performance-based seismic design of CWs are reviewed. The future developments and research tasks of the building CW are also addressed.

2. Acceleration demand

Acceleration demand of the CW relates to the seismic design force and corresponding parameters in current code provisions. For a general CW system (e.g., thin glass CW), the calculated seismic force is smaller than the wind load, while for stone cladding, and large glass panel in tall buildings, the seismic force can be larger. Almost in every seismic design provision, seismic design approaches of the general NCs are directly applicable to the CWs. The equivalent inertia force calculation methods are given in many current codes, e.g., Eurocode [49], New Zealand seismic design code [134], British standard [139], ASCE 7–10 [5], Chinese national code [96], Shanghai local seismic code [124], etc. Due to limited space of this paper, seismic provisions of ASCE 7–10 [5] is listed only. The relevant seismic calculation parameters in some widely used codes are reviewed and discussed.

2.1. Seismic force calculation

The design provisions in the ASCE 7–10 [5] evolved from the 1994 NEHRP provisions [33]. The main contributor for the new provisions was the Building Seismic Safety Council (BSSC). According to the code, the seismic design forces of the NCs (including CWs) are calculated as follows:

$$0.3S_{DS}I_pW_p \le F_p = \frac{0.4S_{DS}a_p}{R_p/I_p}\left(1+2\frac{z}{h}\right)W_p \le 1.6S_{DS}I_pW_p \quad (1)$$

where F_p is the seismic design force applied at the center of gravity of the NC, I_p is the component importance (CI) factor, which takes a value of 1.0 or 1.5, W_p is the component operating weight, a_p is the component acceleration amplification (CAA) factor, which varies from 1.0 to 2.5, the parameter $0.4S_{DS}$ corresponds to the factored mapped design spectral response acceleration at short periods, z is the average height of the NC over the grade, h is the average height of the roof level over the grade, R_p is the component response modification (CRM) factor, it was slightly modified in comparison to the values included in the previous version of the code such that $F_{pNEHRP1994} \approx F_{pNEHRP1997}$ [14]. In the current version of the code, the R_p factor, as defined in section 2.1.2, varies from 1.0 to 5.0. The relationship which involves the a_p term [4,5] was simplified and replaced by a factor $(1+2z/h)$ (floor acceleration amplification (FAA) factor). The adjustment of this factor came from the examination of additional building motion records associated to strong motions with peak ground accelerations greater than 0.1g. According to this distribution, the floor accelerations within the building vary linearly from $0.4S_{DS}$ at grade to $1.2S_{DS}$ at the roof level. Additionally, the dependence of the input acceleration on the fundamental period of the primary system, considered in NEHRP 1994 through the structure-response acceleration coefficient A_s [33,4], was removed, according to observations of records obtained for buildings with long natural periods [28,29].

The upper and lower bounds of the seismic design force F_p are intended to ensure a minimum design force, consistent with the values formerly used by practitioners, and considered in the previous versions of the provisions. No recommendations are given for the vertical component of the seismic design force.

2.2. Codified acceleration demand parameters

As a NC, the seismic design force of CWs involves the equivalent static force initiated by the floor responses of the main structure. In the past decades, the force based seismic design was very popular in code specifications and guidelines. Due to the fact that acceleration demands are represented by equivalent static forces, researchers paid more attention to the acceleration response for a long time. Even nowadays, the specifications of how to calculate the magnitude of the inertia forces are still the most important part in the seismic design of NCs. These methods are also applicable to the CW system. Most current code provisions involve four parameters, i.e., FAA, CAA, CI, and CRM. Floor response spectrum profile is introduced by AC156 [71] for seismic design and testing of the acceleration sensitive NCs.

2.2.1. Floor acceleration amplification (FAA) factor

In the specified calculation procedure of the equivalent static seismic design force for the NCs, FAA factor is considered in most codes. The FAA factor can be derived from the natural earthquake records or numerical analysis of the structures [47]. The peak value and description of FAA specified in various codes are listed in Table 1. From this table, it is shown that only the New Zealand code [134] provides a bilinear distribution profile, while the other codes provide linear profiles. All the recommended FAA factors reach the peak values on the roof where the amplification effect is the highest. However, in practical engineering design of the CWs, it would be very complicated to use the recommended distribution profiles to calculate the seismic force. Thus, engineers usually use the peak FAA factor. In the design code of China, FAA = 2.0 is proposed in the calculation of the dynamic amplification factor [124].

The roof response will depend on spectral shape of the ground motion and the building's dynamic properties. [102,136,127,128] suggested that, for taller structures, the amplification may vary significantly with height due to higher mode effects. Records obtained during the 1994 Northridge earthquake in multistory buildings showed that floor peak horizontal accelerations were generally greater than those recorded at the ground level [61]. FAA reported by Hall [61] for 25 multistory buildings ranges between 1.1 and 4.6. These results are in

Table 1
Floor acceleration amplification (FAA) factor in code provisions [86].

Code	Description	Peak FAA
NEHRP1994/UBC1997	$1+3h_x/h_r$	4.0
NEHRP1997/IBC2006/ ASCE/SEI 7-05	$1+2z/h$	3.0
[13]	$K_1=1+2.33z/h$	3.33
EC8 (BS EN 1998-1:2004)	$1+z/h$	2.0
NZS 1170.5:2004	$C_{Hi}=1+10h_i/h_n$ for $h_i < 0.2\ h_n$ $C_{Hi}=3.0$ for $h_i \ge 0.2\ h_n$	1.0 for $h_i < 0.2\ h_n$ 3.0 for $h_i \ge 0.2\ h_n$ [buildings taller than 12.0 m]
CSA-S832 2006	$A_x=1+2h_x/h_n$	3.0
GB50011-2010/ J12028–2012	$\zeta_2=1+z/h$	2.0
ASCE/SEI 7-10	$1+2z/h$	3.0 or a_i obtained from response spectra procedure
BS ISO 13033-2013	$1+\alpha z_i/h$	3.5

Notes: h_x, z, z_i, h_i = average height of NC above grade level; h_r, h = height of roof above grade level; h_n = height from base of the structure to uppermost seismic weight (mass); a_i = acceleration at the i-th level of the structure normalized by peak ground acceleration (PGA); $\alpha \le 2.5$ is a parameter that is a function of the type of lateral load resisting system.

agreement with those summarized by Soong et al. [132] for data also obtained in the same earthquake. In 2011 Great East Japan (Tohoku) earthquake, floor motions of the two tall buildings situating in Kogakuin University were observed [80], the results showed that the largest FAA is 3.8 in the roof level. FAAs derived from the database of the California Strong Motion Instrumentation Program show that current code provisions can't make a good estimation [51]. Huang et al. [64] also reported that the FAA on the roof level of a tall building can be very high under low or moderate level earthquake excitations, and it may exceed 10.0 due to the whiplash effect. For the CWs located below 60% of the structural height 0–0.6h), FAA is recommended as 5.0, while it can be taken as 6.0 for the upper 40% of the structural height (0.6h to 1.0h). It is noted that elastic response of a structure result in high magnitude of FAA. When the excitation level increases the amplification goes down, sometimes significantly, due to plastic deformations in the structure and/or increased damping.

2.2.2. Component acceleration amplification (CAA) factor

In most commonly used code provisions [134,139,49], the CAA factor (a_p) represents the dynamic amplification (or the resonance factor) of component responses as a function of 1) the fundamental periods of the structure (T) and NC (T_p), 2) the NCs damping ratio, 3) the general configuration of the NCs, 4) the method of attachment of the NCs to the building structure, and 5) the inherent damping and degree of inelastic behavior of the building structure which are dependent on the severity of the ground motion.

Dynamic amplification occurs where the period of a CW closely matches that of any mode of the supporting structure. However, this effect may not be significant depending on the ground motion. For most buildings, the primary mode of vibration in each direction will have the most influence on the dynamic amplification for the CWs. For long-period structures (such as tall buildings), where the period of vibration of the fundamental mode is greater than 3.5 times of T_p, higher modes of vibration may have periods that more closely match the period of the CWs. For this case, it is recommended that amplification be considered using such higher mode periods in lieu of the higher fundamental period. This approach may be generalized by computing floor response spectra for various levels that reflect the dynamic characteristics of the supporting structure to determine how amplification will vary as a function of the NC period. Calculation of floor spectra can be complex, but simplified procedures are presented in [13]. Consideration of the nonlinear behavior of the structure greatly complicates the analysis.

Many current code provisions list simple values of the CAA factor for seismic design of the NCs, however, most of the provisions do not have specific factor for the CWs. Thus, the CAA factors have to be determined by assuming that the CW is a type of normal exterior wall or building envelope (Table 2). The magnitude of CAA varies from 1.0 to 2.5. Except UBC1997 [72], it is obvious that almost all US codes ignore the amplification effect of the CW [5,6,27,28,30,31,33,68,69,70]. Since 1997, there is almost no change in the determination of the CAA for exterior wall elements, including glass CW system. As a result of the lack of supporting research, engineering judgement and practical experience are needed to find a suitable CAA. However, the Chinese code simply gives a factor of 2.0 [124]. The Eurocode provides a complex equation which includes the equivalent CAA description [49]. For tall buildings, the fundamental periods (T_1) are typically much larger than the period of the CW (T_a), i.e. the ratios T_a/T_1 are possibly close to zero. Consequently, the CAA would be 1.5 [49], which is the same as that in the British code [139]. In this code, the selection of the CAA is based on flexible NCs. It has to be noted that there are no experimental results on the CAA factors reported in published literature, although they have been specified in current code provisions for decades.

Table 2
Code specified component acceleration amplification (CAA) factors.

Code	Description	CAA
ASCE-SEI 7-10/IBC2012	a_p	1.0
UBC1997	a_p	2.5
[13]	K_2	2.0
EC8 (BS EN 1998-1.2004)	$3/(1+(1-T_a/T_1)^2)$	1.5
NZS 1170.5:2004	$C_i(T_p)$	2.0
CSA-S832 2006	A_r	1.0
DGJ08-56-2012	ζ_1	2.0
BS ISO 13033-2013	$k_{R,p}$	1.5

Notes: 1) The structure is assumed tall with long fundamental period T_1; 2) T_a or T_p = fundamental period of the component; 3) EC8 provides a formula to calculate the CAA factor while NZS and CSA provide multi-linear relationships to obtain the CAA factor.

When components are designed or selected, the structural fundamental period is not always defined or readily available. The component fundamental period (T_p) is usually only accurately obtained by shaking table or pull-back tests and is not available for the majority of NCs. Values of a_p are based on component's behavior that is assumed to be either rigid or flexible. Where the fundamental period of the component is less than 0.06 s, dynamic amplification is not expected, and the component is considered rigid. The tabulation of assumed a_p values is not meant to preclude more precise determination of the CAA factor where the fundamental periods of both structure and component are available [46]. The NCEER formulation shown in Fig. 1 may be used to compute a_p as a function of T_p/T [14]. It is also adopted by several guidelines and technical reports [29,31,32]. It is obvious that the fundamental period of the CWs (or general NCs) and the main structure should be known before determining the CAA. However, due to the practical construction measures and various types of the CWs, it is hard to determine these fundamental periods. Moreover, the estimated fundamental period of the main building might be not so accurate for special, complicated tall buildings, sometimes the code provided calculation methods are not applicable to such tall buildings. Furthermore, usually the fundamental period does not control the dynamic property of the structure, herein, this formulation would lose its reliability for buildings whose vibration characteristics are controlled by higher modes. Finally, the location of the CWs is not a factor in the formulation shown in Fig. 1. In general, the CAA is larger for the CWs in the higher levels of the building. The unified CAA value is conservative for the CWs (or general NCs) in the lower stories, but could be underestimated in the higher stories.

2.2.3. Component importance (CI) factor

Performance expectations for NCs are often defined in terms of the functional requirements of the structure to which the components are

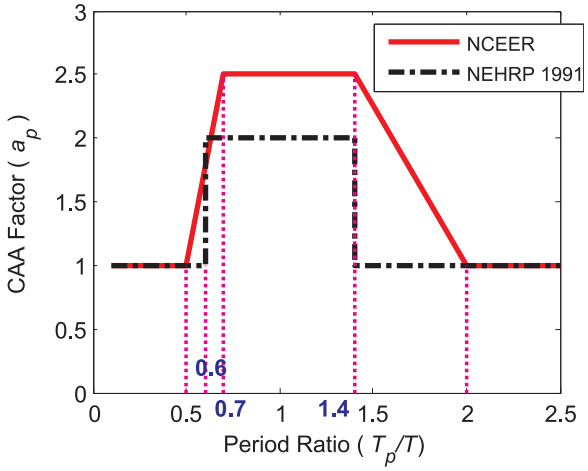

Fig. 1. NCEER formulation for amplification factor [14].

Table 3
Component importance factor (CI).

Code	Description	CI
NEHRP1994	I_p	1.5
UBC1997	I_p	1.5
NEHRP2000/NEHRP1997/IBC2000/ IBC2006/ ASCE/SEI 7-05/ NEHRP2003/IBC2012/ASCE/SEI 7-10	I_p	1.0 or 1.5
[13]	I	2/3
EC8 (en.1998.1.2004)	γ_a	1.0
NZS 1170.5:2004	R_p (Risk factor)	1.0
CSA-S832 2006	I_E	1.0
DGJ08-56-2012	γ	1.4
BS ISO 13033-2013	$\gamma_{n,E,p}$	2.0

Note: CI values are based on assuming the CW system is installed on important tall buildings.

attached. While specific performance goals for NCs especially CWs have yet to be defined in building codes, the component importance (CI) factor (I_p) implies performance levels for specific cases. For noncritical NCs (those with an importance factor, I_p of 1.0), the following behavior is anticipated for shaking with different levels of intensity: 1) Minor earthquake – minimal damage, not likely to affect functionality, 2) Moderate earthquake – some damage that may affect functionality, and 3) Design earthquake – major damage but significant falling hazards are avoided, likely loss of functionality.

Code provisions on the CI factor mostly indicate that it ranges from 1.0 to 1.5, sometime only the two boundary values are recommended (Table 3). For the importance factor of the NCs, most US codes adopt the same factor of the main structure, without considering the functions of the NCs themselves. Taken the US codes for example [5,28–31,68,69,70], CI could be 1.5 if the main structure belongs to risk category IV, but 1.0 if not. Even if the main structure is an important tall building, it is still insufficient to determine the CI factor. The Japanese code [13] provides smallest value, i.e., the seismic importance of the NC is less than that of the main structure. On the contrary, the Chinese code simply gives a value of 1.4 without considering the function of the main building [124]. The most detailed code in that regard is the BS ISO 13033-2013 [139] where the establishment of the CI involves both functions of the building and the NC system with values ranging from 0.8 to 3.0. The CI specification in other codes does not list CW as an important NC system, thus it is assumed to be 1.0.

The CI factor intends to represent the higher importance of life-safety of the NC and of hazard-exposure of the structure. It indirectly influences the survivability of the NC via the required design forces and displacement levels as well as the NC attachments and detailing. While this approach provides some degree of confidence in the seismic performance of a NC, it may not be sufficient in all cases. For example, individual glass panels may break causing a serious falling hazard and termination of their function as a building envelope even if the CW were designed for larger forces. For higher confidence in performance, the NC should be classified as a designated seismic system, and, in certain cases, seismic qualification of the NC or system is necessary.

2.2.4. Component response modification (CRM) factor

The component response modification (CRM) factor addresses the nonlinear action of the NC, e.g. CW. The seismic force demands of a NC (or CW) may be reduced by its damping, ductility, over-strength, and connection details that influence the dynamic response. The expression of the response modification factor varies among the code provisions. To simplify the seismic design procedure, some codes specify the transformation or the alterative expressions to get the CRM factor. Equivalent CRM value from current code provisions ranges from 1.0 to 3.33 (Table 4). In many US codes, except the NEHRP1994 [33], it is listed together with the NC amplification factor according to the type of the NCs [5,28–31,68,69,70]. Among the codes, only the Chinese code [124] specifies the compatible CRM for design of CWs, but it is still short of having solid analytical or experimental basis. The CRM of CW systems involving the amplification effects of the panel, supporting system, and anchorage is rarely studied in the past. Thus, experimental and analytical studies are needed for better understanding of the CRM.

Table 4
CRM factor.

Code	Description	CRM
NEHRP1994	R_p	1.5–6.0
UBC1997	R_p	3.0
NEHRP2000/NEHRP1997/IBC2000/ IBC2006/ACSE/SEI 7-05/ NEHRP2003/IBC2012/ASCE/SEI 7-10	R_p	2.5
[13]	$1/k_0$	$1/0.3 = 3.33$
EC8 (en.1998.1.2004)	q_a (Behavior factor)	2.0
NZS 1170.5:2004	$1/C_{ph}$	$1/0.55 = 1.82$
CSA-S832 2006	R_p	2.5
DGJ08-56-2012	$1/\eta$	$1/0.9 = 1.11$
BS ISO 13033-2013	$k_{D,p}$	1.0 (Low reserve capacity)

2.2.5. Comparisons

Suppose the dynamic factor of a certain glass panel attached at the top of a normal building structure, the dynamic factor (DF) is defined as follows:

$$DF = FAA \cdot CAA \cdot CI / CRM \quad (2)$$

The calculated DFs with the codes discussed in the previous sections are compared in Table 5. From this table, it can be shown that the DF varies among different codes where the British standard [139] is the most conservative (DF = 10.5), while the Canadian code [35] is the least conservative (DF = 1.2). This is due to the different considerations of the four factors that determine the DF. More analytical and experimental studies are needed to justify the existing codes.

2.3. Analytical studies

2.3.1. Closed-form solution

Besides code specifications, analytical studies were conducted where most of the research involved the closed-form solution of the simplified numerical model and the dynamic analysis of simple structures. [43,44,62–131] introduced a continuous beam model to study the effect of the secondary system. [81] proposed a simple method to calculate the dynamic response of a combined primary-secondary system. The considered primary system consisted of a viscous damped uniform cantilever beam, while the secondary system (e.g., CW) was modeled as a damped single-degree of freedom (SDOF) oscillator attached at some point along the height of the beam (primary system, Fig. 2). Both systems were considered to behave linearly. It is important to note that a parametric analysis performed using this method should consider six parameters: oscillator to beam mass ratio,

Table 5
Dynamic Factor (DF) from different codes.

Code	FAA	CAA	CI	CRM	DF
ASCE-SEI 7-10/IBC2012	3.0	1.0	1.5	2.5	1.8
UBC1997	4.0	2.5	1.5	3.0	5.0
[13]	3.33	2.0	2/3	3.33	1.33
EC8 (BS EN 1998-1.2004)	2.0	1.5	1.0	2.0	1.5
NZS 1170.5:2004	3.0	2.0	1.0	1.82	3.30
CSA-S832 2006	3.0	1.0	1.0	2.5	**1.2**
DGJ08-56-2012	2.0	2.0	1.4	1.11	5.05
BS ISO 13033-2013	3.5	1.5	2.0	1.0	**10.5**

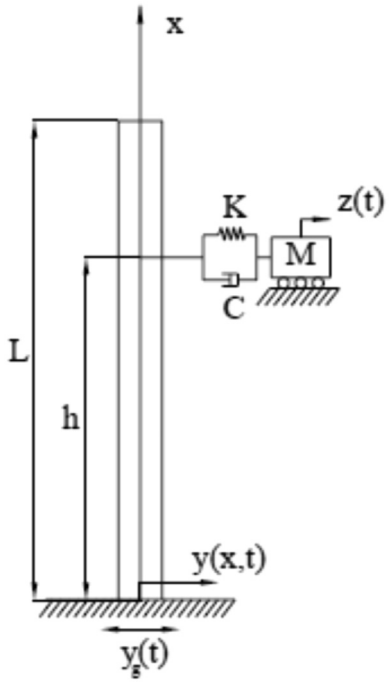

Fig. 2. Single continuous beam model [81].

natural frequencies and damping of the oscillator and continuous beam, and location of the oscillator along the height of the building. One limitation is that the method is only applicable to linear structures.

Another simple method to estimate floor acceleration demands in multistory buildings has been used by [103,102]. A linear multistory building is modeled as a combination of continuous shear and flexure beams with variable stiffness, as shown in Fig. 3. The advantage of this method is the simplicity of the concepts involved, serving as a fast and efficient tool for preliminary estimation of expected demands. Note that for the case of constant stiffness, the response depends only on the first three parameters. Numerical analytical results by the past researchers indicate that the use of only the three first modes, leads to good estimations of acceleration demands [102,136]. The major limitation of the method is its dependence on specific ground motions and its application to buildings exhibiting linear or almost linear responses.

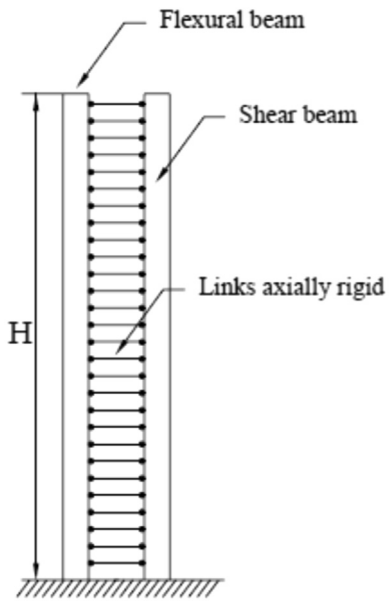

Fig. 3. Simplified double-beam model of multistory building [103].

Moreover, this model neglects the dynamic interaction between primary and secondary systems. Finally, the acceleration demand acquired from this model is hard to consider for the CW system on tall building structure.

Besides the above two main analytical methods, some simplified methods are proposed to estimate the acceleration of the NCs. [118] used a modal superposition approach modified to account for the inelastic response of the primary system. [143,142,144] proposed a simple approximate method to examine the seismic force demands on nonlinear light multi-degree of freedom (MDOF) secondary systems attached to one or two levels in multistory nonlinear buildings. The conventional ground response spectrum technique is used to evaluate the design forces on the secondary system. Dynamic properties (vibration frequencies, modal shapes, and damping ratios) of the primary and secondary systems are attained independently.

2.3.2. Real structure analysis

Sankaranarayanan [122] conducted floor acceleration response analysis of stiff and flexible frame structures with 3, 6, 9, 12, 15, and 18 stories subjected to a set of 40 far-field ground motions. The SDOF NC was assumed to have small masses compared to the total mass of the supporting structure. Acceleration response modification factor was proposed to quantify the reduction in the CAA factors and the inelastic floor response spectrum that was achieved due to the inelastic behavior of the building. However, the results of the study are applicable to regular moment-resisting frame structures. As for CWs on tall buildings, more specific analysis needs to be conducted.

Taghavi [137] estimated the floor acceleration demands in multistory buildings (two generic buildings and four instrumented buildings). Results show that the variation of peak floor acceleration (PFA) along the height of the building is strongly influenced by the fundamental period, lateral stiffness of the buildings, and even the selected the ground motions. For flexible components, FAA could achieve 5.0, while it is specified as 2.5 by some code provisions. Response spectrum method is also involved for the estimation of the PFA and it is helpful to have representative floor response spectrum for the seismic design of CWs or general NCs.

Joseph et al. [74] created three post-Northridge SAC 3-, 9-, and 20-story steel moment frame office buildings that were designed for the Los Angeles area [60], and one 3-story hospital building was designed to help generalize the findings to current design criteria. A suite of 21 ground motions were selected from the PEER-NGA Database [108] using the criteria prescribed by the ATC-63 project [52]. It was found that the current code equations overestimate the PFA/PGA ratio (equals to FAA) in elastic buildings with natural periods between 1.0 and 4.0 s by as much as a factor of 4. A constant FAA factor cannot capture the variation of accelerations of NCs located throughout the height of the supporting structure.

Chaudhuri and Hutchinson [115] analyzed eight representative stiff and flexible steel moment frame buildings of heights 4, 8, 12, and 16 stories. Evaluating the PFA of the nonlinear frames, it was observed that code-specified profiles overestimated the PFAs in nonlinear frames with long fundamental periods. For stiff frames with short fundamental periods, the code-specified profiles may underestimate their absolute acceleration response at the lower floor levels. Moreover, the nonlinear behavior of the frame members generally reduced the PFA as anticipated, however, in other cases, this effect may increase the PFA significantly.

3. Drift demand

Unlike the acceleration demand discussed above, drift demand attracts few attentions of the researchers. Thus, the drift limits (usually interstory drift ratio, IDR) to the CW are relatively simple in current code provisions.

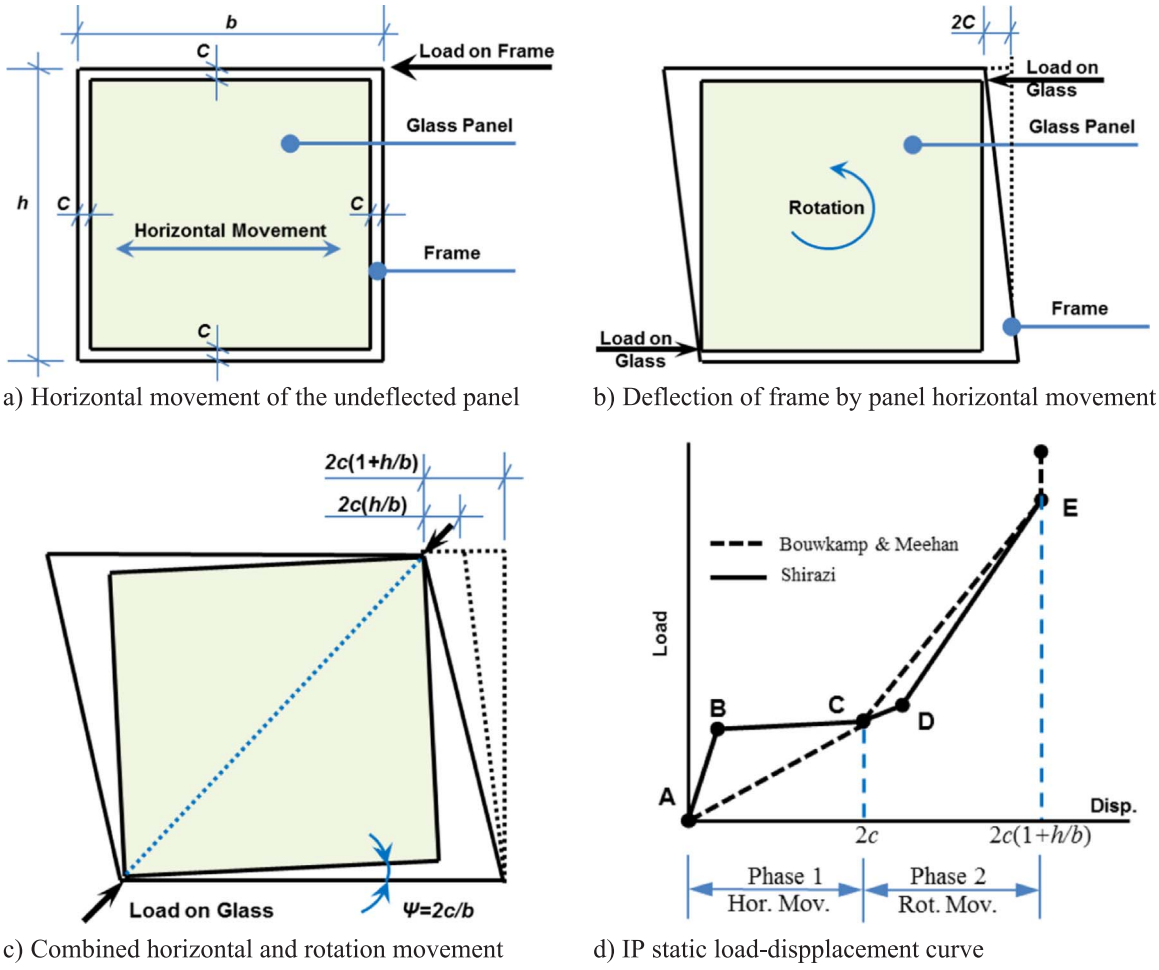

Fig. 4. IP drift mechanism of the framed CW [125,23].

3.1. In-plane (IP) drift mechanism

For the framed glass CW, interstory drift causes the relative movement between the glass panel and the aluminum frame (Fig. 4). The initial gap between the edge of the glass panel and the frame allows small drifts before the direct contact takes place. In this case, the stresses in the glass panel are induced by the friction forces between the panel edges, plastic gaskets, side blocks, or silicon glue sticks. The deformation of the gasket tends to absorb the kinetic energy and buffer the impact velocity. However, once the gasket or the silicon stick were damaged, or extruded out of the frame, direct contact of the glass panel and the aluminum frame will occur causing rapid increase of the stresses in the glass panels at these contact points. Cracks might be generated once the local stress exceeds the critical stress of the glass panel. To understand the contact mechanism, Bouwkamp and Meehan [23], and Sucuoglu and Vallabhan [135], developed a calculation method for the frame drift corresponding to partial and full contact of the glass panel and the frame. The total lateral deformation of the glass panel due to rigid body motion in the frame is expressed as:

$$\delta_r = 2c\left(1 + \frac{h}{b}\right) \tag{3}$$

where δ_r is the lateral drift of the panel, c is the gap between the glass panel and the frame, and h and b are respectively the vertical and horizontal clear distances of the frame. Moreover, Bouwkamp and Meehan [23] conducted a series of IP testing of the framed glass windows and the acquired standard load-displacement curves had three branches (Fig. 4d): 1) The movement of the glass panel, 2) The rotation of the panel, and 3) The combined deformations. The magnitude of the failure load completely depends on the stress concentration close to the contact area between frame and glass panel. Shirazi [125] provided a four-branch load-displacement curve (Fig. 4d). The displacement is very small in the first branch and the physical contact occurred in the second branch. By increasing the drift, the contact of the glass panels and the frame occurs where both vertical and horizontal members of the frame contact the glass corners at opposite sides of the diagonal corners of the frame. After full contact, the stiffness of the CW glass increases and finally the glass cracks. Obviously, Shirazi's model (2005) describes the contact mechanism of the glass panel and frame in more detail than that of the model by Bouwkamp and Meehan [23]. However, both models demonstrated that the direct contact of the frame and glass panel actually increases the stiffness of the CW. Identical observations were found by Sassun [123]. These studies are valid when the glass panel of the framed CW system is glazed with a soft sealant which permits the relative motion of glass plate with respect to the window frame. Once the sealant hardens by aging, the lateral drift capacity of the window panels reduces significantly. However, the neoprene gaskets should have sufficient resilience to permit relative motion of the glass plates in the frames.

For the point supported glass CW, due to its structural layout being different from the conventional frame glass CWs, instead of aluminum frames, it is fixed by the spider arms via the bolt fittings. Its drift curve under IP load is almost linear without any visible change of slope [130]. The IP displacement is absorbed by the rigid-body rotation of the spider arms and the rigid-body translation is facilitated by built-in oversized holes of the bolts between the spider arm and the structural support frame connections, and by the deformations and yielding of the spider arms. Results show that these three mechanisms (Fig. 4a to c)

Table 6
Interstory drift ratio (IDR) in different code provisions.

Code	Description	IDR	Intensity Level
ASCE/SEI 7-10	$D_{pI}=D_p\ I_e$	0.0225	Design
EC8 (BS EN 1998-1.2004)	–	0.0075	Damage limitation
NZS 1170.5:2004	$\delta_{ui}/span$	Max ($span$/250, 2×*glass clearance*)	Serviceability
CSA-S832 2006	–	0.02 = 1/50	Design
DGJ08-56-2012/ GB/ T21086-2007 [38]/ JGJ102-2013	$\Delta_u/h \times 3$	1/500×3 = 1/167	Design

Notes: The *span* in NZS is the story height for the CWs attached to the building and the *glass clearance* is the width of the silicone glue bar inserted on each side of the glass panel (common width = 10 mm). D_p, δ_{ui} & Δu are calculated relative displacement of the neighboring stories, and I_e in ASCE is the building importance factor.

contribute 19%, 57%, and 24%, respectively.

The drift mechanism depends on the structural configuration of the CW systems. For the dry glazed CWs fixed by the chemical anchor bolts, steel angles, steel cables with spiders, and C-shape aluminum anchors, further studies are necessary to define the IP drift curves. Moreover, for the structural silicon glazed CWs, the mechanical properties of the sealant should be understood comprehensively to define its contribution to the IP drift profile under the action of the story drift induced by earthquakes. Experimental results have shown that the drift and fallout capacity of the structural silicon glazed CW is 146% and 54% larger than that of the dry glazed CW [25,94]. On the other hand, the behavior of the out-of-plane (OP) vibration of CW systems was rarely studied. This is related to the OP CAA factor and is useful in calculating the equivalent seismic force of the CW.

3.2. Codified interstory drift ratio (IDR)

Almost all the current code provisions specified IDRs for various structural types of the major building types. The codified IDR values for buildings no less than 250 m in height are listed in Table 6. In British standard [139], building cladding (including CW system) is assumed to be the drift sensitive NCs. The story drift should reflect the inelastic behavior of the structure (best estimate of actual building drift at the ultimate limit state), but it does not provide any drift limit in the code. In the Chinese code for design of CW [124,97], however, it recommends that the IP peak drift of the CW should be no less than three times the elastic deformation limit of the main structure. The deformation limits of the main structure are specified both in China national seismic design code and Shanghai local seismic design code [140,95,96]. The Canadian code gives a value of 0.02 for any structural types [35] and it is conservative for many building types. It is known that once the glass panel is broken, it loses its function immediately. This phenomenon corresponds to the serviceability limit state mentioned in the New Zealand code [134] where the drift limit corresponds to this condition. It should be noted that regarding the structural height, a drift modification factor is specified for the ultimate limit state where for buildings higher than 30 m, the modification factor is 1.5 [134]. The Eurocode [ECS, 2004] provides drift limitations for a building having ductile NCs, but it does not provide specific provisions for the deformation ability of the CW where it is implied that the CW has to endure this drift limit. ASCE 7–10 [5] lists detailed procedure for the calculation of the relative displacement within a structure, D_{pI}, as the product of the importance factor, I_e, and the calculated relative displacement of the neighboring stories, D_p, i.e.

$$D_{pI} = D_p I_e \tag{4}$$

$$D_p = \Delta_{xA} - \Delta_{yA} \tag{5}$$

where Δ_{xA} and Δ_{yA} are the allowable drift at the respective levels x to which upper connection point is attached and y to which lower connection point is attached. Alternatively, D_p is permitted to be determined using modal procedures from the difference in story deflections calculated for each mode and combined by an appropriate modal combination procedures. It should be less than:

$$D_p = \frac{h_x - h_y}{h_{sx}}\Delta_{aA} \tag{6}$$

where Δ_{aA} is the allowable story drift of the structure, h_{sx} is the story height used in the definition of allowable drift Δ_a [5], and h_x (h_y) is the height of level x (y) to which upper (lower) connection point is attached. Suppose the building belongs to risk category IV, the allowable drift limit should be 0.015×1.5 = 0.0225. It actually falls between the former specifications of FEMA 273 [27], 0.03 for life safety performance level, and 0.01 for immediate occupancy performance level.

From Table 6, it is shown that US and Canadian codes have the largest drift demand, while the Chinese code results in the lowest value. Actually, the drift demand relates to the physical parameters of the main structure, such as the building height, structural type, and ground motion. Huang et al. [64] indicated that the code-specified inelastic story drift limits were larger than the specified three times the corresponding elastic drift limit in the same code. Furthermore, even for one tall building, the height-wise story drift distribution along the building was actually not uniform. In contrast to the multistory buildings, the largest drift usually occurs near the mid-height of the structure due to the higher mode effects. In this case, Huang et al. [64] recommended a three-branch drift demand relationship along the building height where the largest drift demand is 1/50 (0.02), which is equal or close to Canadian and US codes [35,5], respectively. Moreover, the seismic fallout drift for the glass CW should meet the relative displacement requirement [5]:

$$\Delta_{fallout} \geq 1.25 I_e D_p \tag{7}$$

or 0.5 in. (13 mm), whichever is greater, where $\Delta_{fallout}$ is the relative seismic displacement (drift) at which glass is expected to fall out from the CW and shall be determined in accordance with AAMA 501.6 [2] or by engineering analysis. This indicates that the drift capacity of the CW should be no less than the demand IDR of the main structure with 25% redundancy. It is noted that the code provisions for the IDR factor are mostly derived from limited numerical analysis of multistory buildings without specifying provisions on the floor drift spectra for the CWs.

3.3. Analytical studies

Based on the solution of the problem for nondispersive damped waves in a one-dimensional continuous medium [45], the shear strain is used in a continuous shear beam with uniform stiffness as an analogy to the IDR in a building structure [73]. The closed-form solution of the IDR is thus developed in terms of dimensionless height, fundamental period, and damping ratio. Miranda [103] presented an approximate method to estimate the maximum IDR in multistory buildings subjected to earthquake ground motions. In this method, the multistory building is modeled as an equivalent continuum structure consisting of a combination of flexural and shear cantilever beams. However, the approximate method is intended to be used during the preliminary design of new buildings and for a rapid evaluation of existing buildings. It is not meant as a substitute of more detailed analyses. Miranda and Reyes [101] extended this method to be applicable for the buildings with non-uniform height-wise lateral stiffness. On the basis of the above two methods, Akkar et al. [1] presented an improved procedure by using the beam-column stiffness ratio where the estimation accuracy of the drift demands was increased compared to the former methods [1999,2002]. Krawinkler [59] developed a procedure to estimate the drift demands of 3-, 9-, and 20-story steel moment resisting frame

structures. They observed that the roof and maximum IDR depend strongly on the height of the structure and that the height-wise distribution of the story drifts are strongly related to the ground motion and the principal structural properties. The same building structures were studied by Lin and Miranda [82] and approximate approaches were developed for estimating the maximum roof displacement. The story drift demands of the planar regular X-braced steel frames were analyzed by Karavasilis et al. [76], but the relevant drifts were not suitable to investigate the building envelope such as CW system. Nonlinear time history analysis of regular moment frame structures subjected to ordinary ground motions were conducted by Medina and Krawinkler [90] where regression analysis methods were provided to evaluate the height-wise IDR distribution profile. Besides the maximum IDR during the earthquake excitation, the residual drift demands might cause damage to the CW system. Incremental dynamic analysis of generic frame models showed that the amplitude and height-wise distribution of the residual drift demands strongly depend on the frame mechanism, the height-wise system structural over-strength, and the component hysteretic behavior [2006].

Height-wise distribution of the IDR is useful to determine the location of the soft story of the primary structure, but it cannot represent the frequency contents of the floor motions. However, drift spectrum can display the relationship of the spectral IDR and the fundamental period of the NCs attached to the neighboring floors. Instead of a SDOF system model, [73] used the linear continuous shear-beam model to estimate the drift demand spectrum of the simplified building structure. The proposed procedure is proven to be more accurate than that derived from traditional response spectrum. Chopra and Chintanapakdee [41] indicated that the discrepancies between the drift and response spectra simply reflect the higher-mode responses. Accordingly, the response spectrum analysis is preferable to obtain the drift demand spectrum of the structure because it represents standard engineering practice and is applicable to a wide range of structures. In order to eliminate the unexpected residual drifts generated by Iwan's model [73], Kim and Collins [78] examined the physical and mathematical basis of Iwan's simplified shear-beam model and internally damped shear-beam model was proposed where the residual drift was finally eliminated. Miranda and Akkar [100] replaced the shear-beam model with the combination of flexural and shear beam model such that the deformation profile of any multistory building can be simulated accurately.

The code-based approximate estimation of the fundamental period according to the height of the structure can reduce the accuracy of the above procedures, including that in [100]. Thus, a standalone approach should be developed to solve this problem. For this purpose, Shodja and Rofooei [126] used a lumped mass beam model to develop a method for estimating the drift spectra of buildings with regular height-wise stiffness distributions. Till now, the above-mentioned procedures of determining the IDR are not yet applied in the seismic design of drift-sensitive NCs. Recently, under the philosophy of displacement-based seismic design of structures [114]. Calvi [34] proposed an approximate method to construct relative displacement floor (drift) spectra, which accounts for the period and inelasticity of the supporting structure to define the shape of the floor spectra using the elastic damping of the supported element in order to define the magnitude of the floor spectra. The required parameters (peak floor displacement and peak ductility demand) can be obtained through a direct displacement-based design assessment of the NCs including CWs.

4. Codified seismic experimental approaches

In this section, current seismic experimental protocols are reviewed. Their applicability for evaluating the seismic performance of the CW system is also discussed.

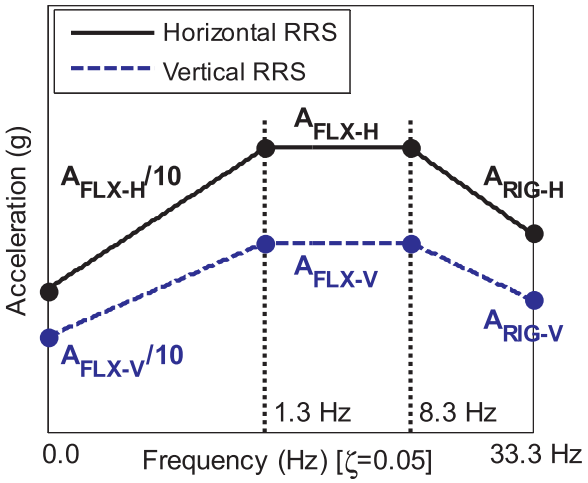

Fig. 5. AC156 recommended spectrum (5.0% damping) [71].

4.1. Shaking table testing

4.1.1. AC156

AC156 [71] is currently one of the basic references for seismic qualification test of NCs, systems and equipment, and for verification of compliance with IBC 2006 [69]. The code specification is applicable to experimental verification of NCs and systems with fundamental frequencies greater than 1.3 Hz. Therefore, this code is applied to the CW satisfying this requirement. The information required by the specification to define the testing histories and the compliance criteria include: the equipment attachment elevation with respect to grade, z, the average building roof elevation, h, the spectral response acceleration at short period, S_{DS}, the equipment importance factor, I_p, a description of the functional requirements of the equipment, and a description of mounting conditions, subassemblies, mass distribution, possible equipment variations, and installation instructions. The Required Response Spectrum (RRS) is derived from the IBC2006 formula for total design seismic horizontal force F_p given in Eq. (1). The spectrum for the vertical component is considered equal to 2/3 of the horizontal ground spectrum. The spectra are defined by the parameters A_{FLX} and A_{RIG}, defined in Eqs. (8) and (9), and shown in Fig. 5.

$$A_{FLX} = S_{DS}\left(1 + 2\frac{z}{h}\right) \leq 1.6S_{DS} \tag{8}$$

$$A_{RIG} = 0.4S_{DS}\left(1 + 2\frac{z}{h}\right) \tag{9}$$

For vertical RRS, z may be taken equal to 0. Alternatively, the horizontal RRS can be constructed from the information obtained during the structural analysis of the building, i.e.

$$A_{FLX} = 2.5A_x a_i \tag{10}$$

$$A_{RIG} = A_x a_i \tag{11}$$

where A_x is the torsional amplification factor and a_i is the acceleration at the i-th level obtained from the dynamic analysis.

Realizations of non-stationary broadband random excitations having a frequency content ranging between 1.3 and 33.3 Hz matching the RRS should be generated. The total duration of the shaking table motion should be no less than 30 s. The minimum duration of the strong motion should be 20 s. Longer strong motion durations are acceptable. Although this code is not proposed specifically for seismic qualification testing of CW systems, it is applicable to CWs satisfying the testing requirements. If necessary, recommended acceleration spectra can be revised based on actual dynamic properties of the CW and the main structure. In British standard [139], a similar floor response spectrum is

recommended for shaking table testing of the NCs.

4.1.2. FEMA 461

The shaking table testing protocol is appropriate for fragility evaluation of NCs whose behavior is sensitive to the dynamic motion at a single point of attachment in a building structure [10,11]. This protocol is not composed for shaking table testing of CWs on the buildings, which has at least two attachment points at neighboring floor levels. However, it offers useful information for testing of CWs. The testing procedure is based on the work by the Construction Engineering Research Laboratory [147]. The first objective of the shaking table testing protocol is to evaluate the seismic response and performance of NCs under simulated floor motions at increasing intensities, and the second objective is to characterize the functional performance levels and the damage states of the component to quantify its seismic fragility. For the sake of achieving the above two objectives, detailed test procedure is recommended comprising of test processes, intensities of shaking, input motions, instrumentation, and monitoring.

In this protocol, the parameter used to characterize the intensity of the input motion is the peak spectral acceleration at the appropriate natural frequency for the specimen and damage state. At least three shaking intensities should be used during testing. The intensities of shaking used for system identification tests should be low enough to avoid any damage to the test specimen. The intensities for performance evaluation should be selected to induce damage states associated with economic losses and downtime. Similarly, in failure tests, the intensity of shaking should be large enough to induce damage states associated with life safety or incipient failure. The input motions consist of 60 s long narrow-band random sweep acceleration records scaled to produce motions which have relatively smooth response spectra. The bandwidth is one third octave and the center frequency of the record sweeps from 32.0 Hz down to 0.5 Hz at a rate of 6 octaves^2/min. It slightly differs from the recommendation of AC156 (3.3–33.3 Hz) [71]. A sweep from high to low frequencies is used to first excite higher vibration modes that have associated failure modes at smaller amplitudes compared to low frequency failure modes. An 80 s long time history and corresponding response spectrum developed by the authors of this paper is shown in Fig. 6. The spectral content of the generated floor motions time history should be predefined to represent the spectral range of the target floor spectrum.

The response spectrum for the vertical component history record is approximately 80% of that of the horizontal component. The testing time instant at which a given damage state is achieved should be recorded in order to identify the center frequency that caused the damage state. The amplitude of motion which caused the damage state is obtained from the test response spectrum, calculated from the shaking table motion up to 10 s prior to the observation of the damage state. The record responsible for the damage state should be notch-filtered considering the frequency and time at which the damage state was observed, in order to remove the frequencies that have already generated a given damage state. The rules for designing the filter are specified in FEMA 461 [10]. The peak value distribution, time duration, and target spectrum need to be studied comprehensively before generating input motion time history for shaking table testing of the CW system.

4.1.3. GB/T 18575

Chinese government provided a shaking table test standard of architectural CW in 2001 [40]. A testing frame is necessary to be designed for installation of the CW specimens, which should have the ability of producing the expected story drift. However, there are no provisions on how to design the frame. Designing a suitable testing frame is a challenging task prior to the test. The CW specimens should be tested at full scale and at least have two vertical story levels and three horizontal glass panels. Typical horizontal and vertical gaps between the neighboring panels and between the adjoining frames

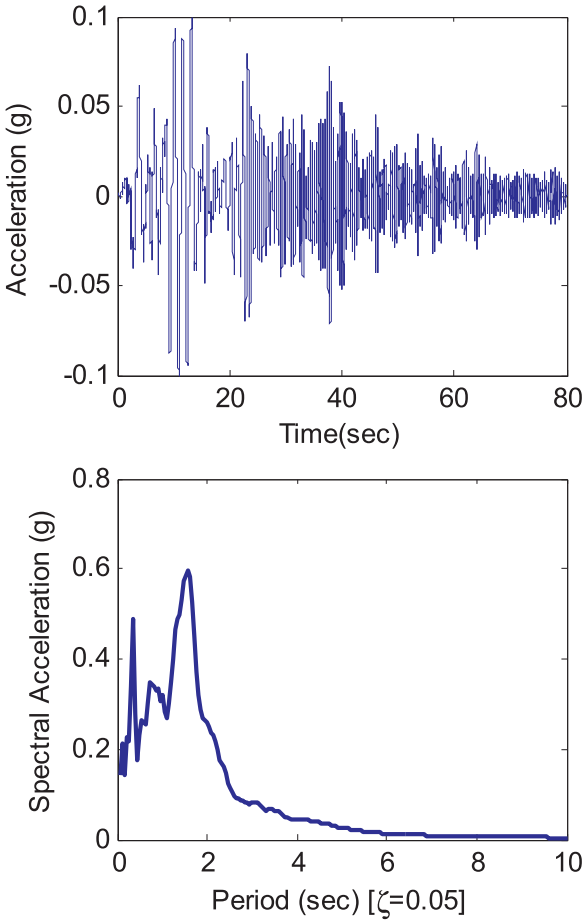

Fig. 6. FEMA 461 compatible time history and response spectrum.

should be included. In order to determine the dynamic properties of the testing system, e.g., the vibration frequency, vibration mode, and damping ratio, white noise with peak acceleration of 0.07–0.1*g* should be input to the testing system before actual tests. The peak acceleration of the input motions should start from 0.07*g* and increase to 0.5 times the design peak ground motion (PGA) in the following testing scenarios. However, the required input motions, which are also known as the core part of the shaking table test, are not yet addressed. In the newest draft standard for reviewing [39], some natural ground motions are recommended if there are no proper motions available. Artificial motions are also acceptable and their selection method should follow the current seismic design code [96]. The code specifications are helpful in shaking table testing of CW systems, but the issues of test frame design, and the selection and/or generation of the input motions are still critical problems to be solved.

Finally, it is worth to mention that the former two shaking table testing protocols (AC156 [71] and FEMA 461 [10]) are very rarely used to investigate the seismic performance of the CW. In China, however, GB/T 18575 was used very often.

4.2. In-plane (IP) racking testing

4.2.1. AAMA 501.4 & 501.6

American Architectural Manufacturers Association (AAMA) specified the laboratory test methods for both static and dynamic testing to evaluate the IP drift capacity of framed glass façade systems [2,3], which was first developed by Behr and Belarbi [18] and named the dynamic crescendo test. Building Components and Envelope Research Laboratory (BCERL, Pennsylvania State University) previously utilized this method for racking tests on CW mock-ups for the static steps. The

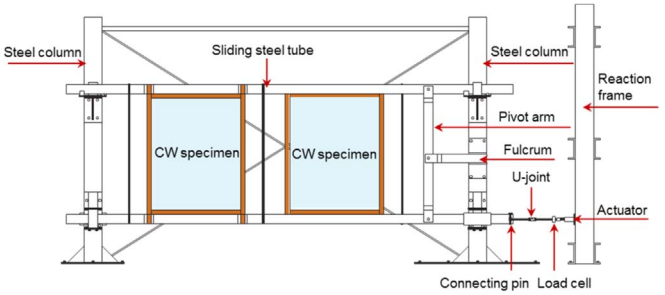

Fig. 7. IP dynamic racking test setup [2].

dynamic and static crescendo tests have the same applied displacement protocols and their main difference is in the magnitude of applied cyclic drift frequencies. The testing facility consists of two tubular steel beams that represent spandrel beams on adjacent stories of a multistory building, Fig. 7. The CW specimens were centered between the sliding steel tubes of the test facility and the vertical mullions were attached at all four corners to the facility's sliding steel tubes. These steel tubes slide on the roller assemblies in opposite directions by means of fulcrum and pivot arm mechanism. The bottom sliding steel tube was displaced by a computer controlled electrohydraulic servo-actuator having a dynamic stoke capacity of ± 3.0 in. (± 76.0 mm). The fulcrum and pivot arm mechanism attached to the top and bottom sliding steel tubes doubled the effective servo-actuator stroke capacity to ± 6.0 in. (± 152.0 mm). This standard test setup in Fig. 7 can be calibrated based on the dimension of the CW systems.

The loading curve consists of a concatenated series of 'ramp up' intervals and 'constant amplitude' intervals, Fig. 8. IP racking displacement steps between constant amplitude intervals should be 6.0 mm. Ramp up intervals and constant amplitude intervals consist of four sinusoidal cycles each. Crescendo tests are performed at a frequency of $0.8+0.1/-0.0$ Hz for total applied racking displacements (drift amplitudes) of ± 75 mm or less, and $0.4+0.1/-0.0$ Hz for total applied racking displacements (drift amplitudes) greater than ± 75 mm. The critical conditions including glass fallout, $\Delta_{fallout}$, and glass cracking, $\Delta_{cracking}$, are defined. This considers the peak drift and frequency content of the story drift time history during earthquakes. However, due to the various structural types, building height, soil site conditions, etc., the specified static test method cannot reproduce the actual full dynamic action imposing on the CWs installing in tall buildings.

4.2.2. FEMA 461

The FEMA 461 [10] proposed a quasi-static racking testing protocol for seismic investigation of NCs including CWs. It assumes that the CW system does not involve the structural analytical models used to predict

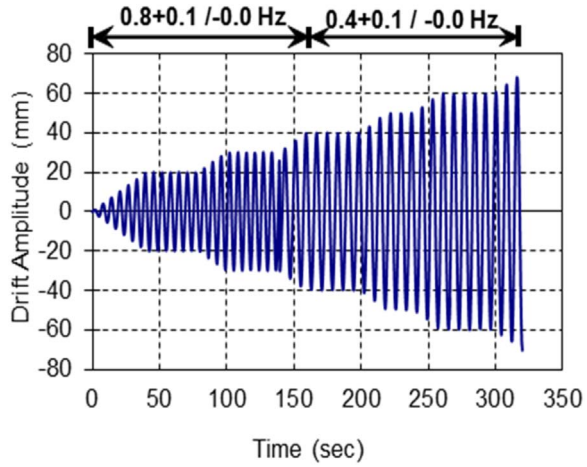

Fig. 8. Schematic of displacement for full crescendo test [65].

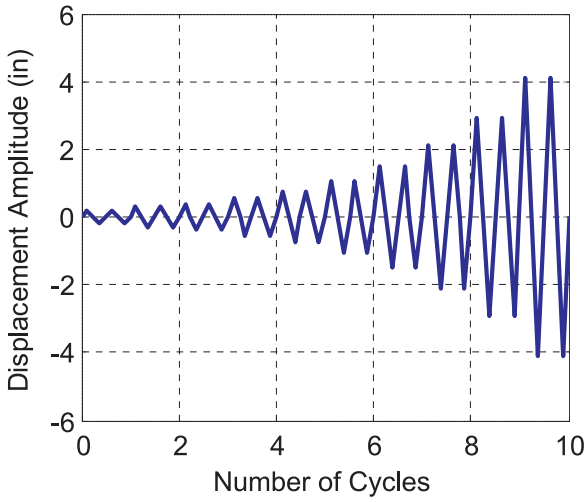

Fig. 9. Displacement loading history [65].

building performance. This racking testing protocol consists of a set of low rate cyclic displacements or forces which follow a predefined pattern. This protocol can also be used for the characterization of the force-displacement constitutive relationships, which is referred to as testing for modeling because it allows for estimating mechanical properties (strength, stiffness, etc.) and low-cycle fatigue properties.

The loading history of the displacement controlled test consists of cycles of step-wise increasing displacement amplitudes which allows for the quantification of one or more damage states. Two cycles at each amplitude are performed, as shown in Fig. 9.

The loading history is defined by the smallest target deformation, Δ_0, corresponding to the minimum deformation amplitude of the testing protocol. It should be less than the minimum displacement capable of inducing the first damage state. A minimum IDR of 0.0015 is recommended. It is also defined by the maximum target deformation, Δ_m, corresponding to the deformation level at which the largest damage state is achieved. It should be estimated before the test. A maximum IDR of 0.03, in absence of more detailed specimen capacity information, is recommended. The number of steps n and amplitude of cycles, a_i, are other characteristics of the loading history. The n parameter should be equal to or greater than 10 and the amplitude a_i of the first and last cycle should be $a_1=\Delta_0$ and $a_n=\Delta_m$, respectively. However, if the final damage state is not observed at the end of the loading history, the amplitude should be increased by using additional increments of $0.3\Delta_m$. Nevertheless, the code recommends continuing with the loading protocol even if the last damage state is achieved. The amplitude a_{i+1} of the displacement history at the $i+1$ step is given by:

$$\frac{a_{i+1}}{a_n} = 1.4\frac{a_i}{a_n} \tag{12}$$

Fig. 9 shows the displacement loading history for the case $\Delta=0.0015$, $\Delta_m=0.03$, and $n=10$. The number and relative amplitude of individual excursions are based on the responses of structures to a set of 20 ground motions records.

In the testing protocol, it is essential that interstory drift is the engineering demand parameter (EDP), controls the behavior of the NC, and triggers the different damage states. An adequate step-wise loading history has to be considered in order to sweep all possible damage states, avoiding the activation of more than one damage state at the same time. The proposed loading protocol history given by Eq. (12) was obtained from statistical analysis of seismic response data of the inelastic SDOF and MDOF systems using engineering judgment. The protocol intends to represent cumulative damage effects, independent of ground motion and the type of NC. No near-fault ground motions were considered in the development, as was the case for the CUREE wood-frame loading protocol [79]. It is assumed and demonstrated that

Fig. 10. UB-NCS facility [117].

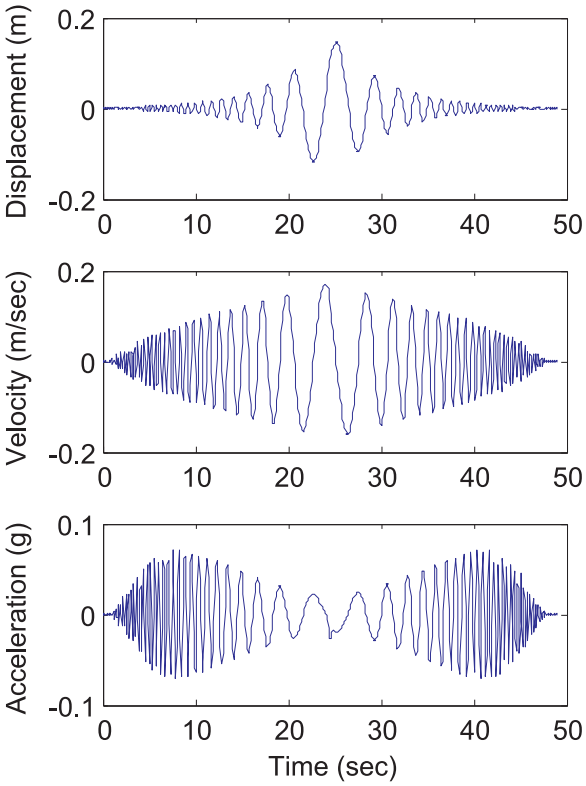

Fig. 11. Parametric testing protocol at bottom level of the CW unit [65].

near-fault motions can generate larger displacement demands in fewer cycles, and thus, they do not control the number and sequence of amplitudes in the loading history. Besides the loading protocol, the commentary section of FEMA 461 [10] introduced some existing test setups for glass CWs, horizontally and vertically attached cladding panels.

4.2.3. GB/T 18250

The IP deformation performance test [56] is a static test procedure. It introduces the specimen setup and the deformation rating method. It is suitable for the framed glass CW. As for the other types of CWs, i.e., stone, point supported, or masonry CWs, the mock-up of the frame and the specimen should be carefully designed to satisfy the actual details.

4.3. UB-NCS testing

The UB-NCS, Fig. 10, testing protocol consists of a pair of displacement histories for the bottom and top testing platforms that simultaneously match: 1) a target floor (or ground) response spectrum, and 2) either a target generalized interstory drift or a maximum interstory drift, based on the anticipated specimen deformation capacity. The input variables for the protocol are the local seismic hazard, in terms of the short and 1.0 s spectral accelerations defined in ASCE 7-05 [2005], the normalized building height above grade where the nonstructural system is located, and optionally, the maximum drift to be imposed. For fragility assessment purposes, this experimental setup has considered a generic site with spectral accelerations $S_{DS}=1.0g$ and $S_{D1}=0.6g$, a generic nonstructural system located at a roof building level, and a maximum drift = 3%. The protocol sweeps frequencies between 0.2 and 5.0 Hz, corresponding to the UB-NCS operating frequency range, which is sufficient to capture the first few modes of vibration that contribute to the seismic response of multistory buildings.

The testing protocol was calibrated to induce/impose the same number of 'Rainflow' cycles [7] on acceleration/displacement sensitive NCs as would be experienced during real building floor motions. The motion time histories exhibit an instantaneous testing frequency transitioning from high to low frequencies, and then back again to high frequencies. The final high frequency sweep is intended to capture possible high frequency acceleration-induced failure modes of nonstructural systems damaged by low frequency interstory drifts. The loading history is the closed-form solution of a continuous cantilever beam model [117]. The model structure has shown promising results in simulating the seismic responses observed in multistory buildings during real ground motions [138]. The closed-form qualification testing protocol time history equations for the bottom level of the drift sensitive NCs were shown in [116]. Based on this method, suppose the story is 13 ft (3.65 m), the parametric testing protocol at the bottom level of the CW is calculated and shown in Fig. 11, and the parametric drift time history is shown in Fig. 12. The recommended protocol is derived from the closed-form solution of the simplified numerical models and generic multistory buildings.

To develop a more applicable IP testing protocol, Hutchinson et al. [67] conducted nonlinear analysis of two low-rise and mid-rise steel buildings using 15 selected ground motions. Considering the structural damage index, four new IP loading protocols were obtained for the 1st

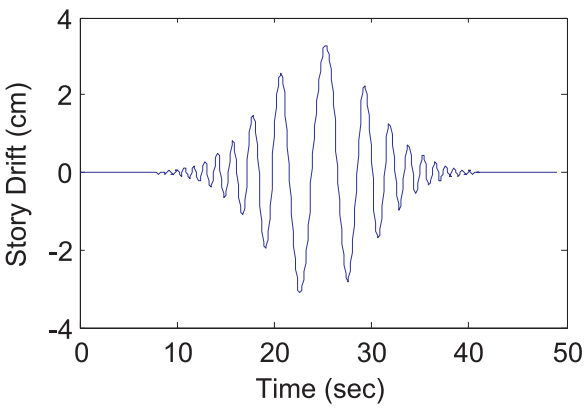

Fig. 12. Parametric story drift protocol [65].

story and the other stories. However, the applicability of the protocols to the CWs in tall buildings is doubtful and more parametric studies are necessary to resolve this issue.

The available experimental approaches are powerful to investigate CW's various seismic behaviors, e.g., shaking table testing is convenient to understand the dynamic properties and responses, IP testing helps us to find the IP drift capacity, UB-NCs testing is the most powerful approach but it has high requirement for the testing facilities. In most cases, preliminary analysis is necessary to determine the proper experimental approach.

4.4. Experimental studies

4.4.1. Shaking table testing

Shaking table testing of the CW (especially the CW in tall and special buildings, or made from novel materials) is very common in China. Since 1994, a large amount of shaking table tests have been conducted to investigate the seismic performance of the CWs. Ma and Yan [88] fabricated a steel frame to simulate the main structure, and a full-scale glass CW unit was installed on the frame. Synthetic and natural ground records were scaled and input to the shaking table as the excitation with ascending peak accelerations. Cao et al. [36] designed a RC frame to simulate the main structure and natural records were input to the shaking table to test the seismic performance of glass CW. Other researchers reported shaking table testing of stone and glass CW systems using identical shaking table test procedures [145,146,83,84].

On the basis of the former studies and a number of shaking table tests of several types of CW, Huang et al. [64] stated that: 1) the input motions of the shaking table test should be based on the floor motions of the main structure, 2) the test frame, whether made from RC or shaped steel, is actually a type of floor motion generation device and does not simulate the main building that the CW being installed on; instead, it generates the required acceleration and story drift responses passed from the neighboring floors, and 3) the seismic evaluation parameters, i.e., the EDPs, should be defined before test, and they represent the evaluation criteria of the seismic performance of the test specimens.

Because the shaking table testing facility (single table) can only reproduce the single point excitation, it is not straightforward to exert earthquake motions from two ends of the CW specimens. Therefore, in order to reproduce the EDPs specified by the code provisions [141,98,99], including the FAA (2.0–5.0) and IDR factors, Lu and Huang [84] indicated that the prime target of the shaking table test of the CWs is to reproduce the codified EDPs (IDR and FAA). Only carefully designed testing frame can reproduce the possible earthquake action and then evaluate the seismic performance of the tested CW unit. This approach is a floor acceleration controlled method. The critical problem of the test is to reproduce the seismic demands, such as accelerations and drifts. Shaking table facility can only provide inertia loading, while the IP drift action is difficult to reproduce at the same time. To overcome this problem, Huang [65] designed a very stiff steel frame to install the glass CWs, a series of IP pre-deformations was exerted to represent the IDR demand corresponding to a certain earthquake intensity level, then the floor motions in OP direction (Fig. 13) were input to the shaking table. The development of the testing method in [85] consisted of 3 steps: 1) The preliminary analysis of the main structure to determine the IDR and FAA demand, 2) Acquiring the representative floor spectrum of the main structure through comprehensive floor response analysis by inputting selected ground motions, and 3) Designing a stiff frame which can reproduce the floor response with negligible acceleration amplification effect. The relative studies were reported in [85,86] as well.

4.4.2. In-plane (IP) racking testing

IP racking testing is the most acceptable approach to investigate the seismic performance of the framed glass CW in the world. To find the coupled OP & IP loading capacity of the CW in multi-story buildings, Thurston and King (1992) tested three types of full-scale three-story framed glass CW by using sinusoidal loading curve. They concluded that IP loading test is qualified to investigate the seismic performance of the CW with recommended testing procedure. However, through the in-plane/out-of-plane (IP/OP) and the in-plane/torsional (IP/T) tests, Behr et al. [20,21] found that for those glass types prone to glass fallout, the fallout rates observed during the IP/OP tests were generally greater than those observed during the IP tests. However, those glass types that resisted glass fallout completely during the 1P tests continued their total resistance to glass fallout during the IP/OP and IP/T tests. The loading frequency varies from 0.5 to 4.0 Hz with five or six cycles per amplitude. Therefore, for the safety issue, the coupled IP/OP and/or the IP/T tests are preferable when the experimental facilities are available. This method was used to evaluate the seismic performance of common types of architectural glass in a typical storefront wall system. Pantelides and Behr [109] conducted a series of IP dynamic racking tests of the CW with various types of glass specimens such as the annealed, heat-strengthened and fully tempered glass in monolithic and laminated configurations. Triangular loading curve with increasing peak displacements was employed to investigate the post-breakage and fallout behavior of different CW glass elements under IP dynamic racking motions. The loading frequencies were 0.5 and 1.0 Hz for different expectations of the glass breakage.

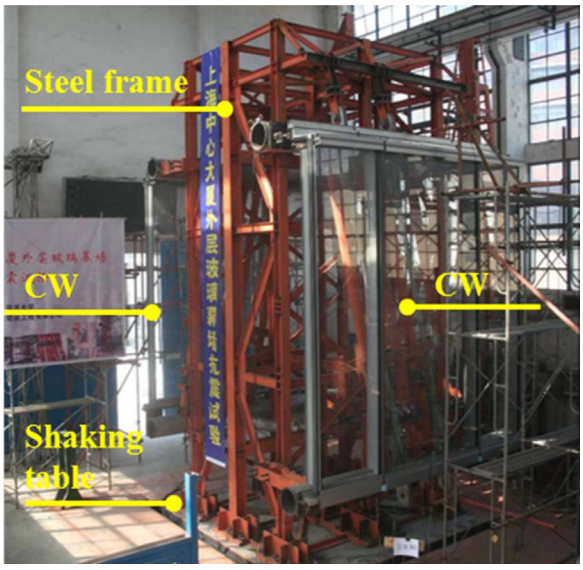

Fig. 13. Shaking table testing of the glass CW [65].

Because of the progressively increasing racking amplitudes at a constant frequency, produces some distinct and repeatable results in terms of identifying IP drift magnitudes associated with predefined seismic limit states for architectural glass. The test method was named 'crescendo tests' [18]. It is a step-shaped swept sine function that has a total duration of just under four minutes. It consists of a continuous series of alternating 'ramp-up' and 'constant-amplitude' intervals, each comprised of four sinusoidal cycles at a nominal frequency of 0.8 Hz. Each drift amplitude step is ± 6 mm. The number of cycles at each step and the test frequency were selected to be representative of drift time histories that could occur in building envelope wall systems under seismic loadings. Experimental applications of this method revealed distinct and repeatable dynamic drift limits related to glass cracking and glass fallout for various types of architectural glass tested in a representative storefront wall system and a representative mid-rise curtain wall system Behr [19]. Many experimental studies were performed to investigate the seismic performance of the CW by using this method [26,91–93].

Besides the framed glass CW, pointed supported glass CW was tested

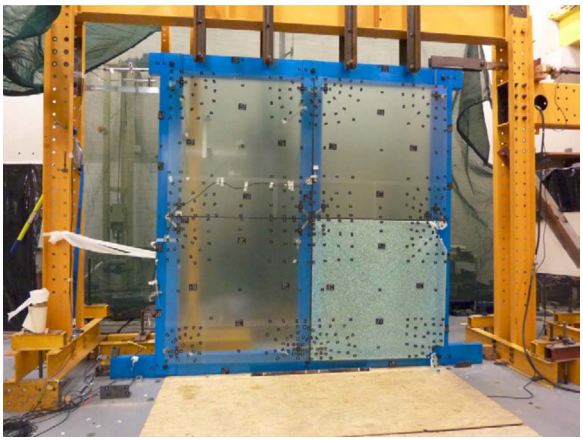

Fig. 14. IP racking testing of the point supported glass CW [130].

[130] by using the recommended testing method [18,3]. The test specimen consists of four 1.2×1.2 m toughened 12 mm-thick glass panels joined with 8 mm-thick silicon weather sealant and connected with spider arms to the support structure. The support frame was fabricated with flange channel sections and bolted together using single snug-tightened M24 bolts to allow the frame to rack as a mechanism (Fig. 14). Results showed that the glass panel rigid-body translation at the oversized connection holes, spider arm rotation, and plastic deformations in the spider arms allowed the system to move laterally and created the increased drift capacity.

As for the UB-NCS testing protocol, it has been used for seismic testing of the hospital facilities [116], steel-studded gypsum partition panels [106], etc. but never for the CW, relevant pilot study is necessary.

5. Performance-based seismic analysis

5.1. Performance levels

The Pacific Earthquake Engineering Research (PEER) Center has developed a PBEE methodology (referred to as the PEER PBEE), which consists of four successive analyses: hazard, structural, damage, and loss [58]. The methodology focuses on the probabilistic calculation of meaningful system performance measures to stakeholders by considering these four analyses in an integrated manner, where uncertainties are explicitly considered in all analyses. PEER PBEE methodology combines these probabilities in a consistent manner using the total probability theorem, where the end result is the probability of exceedance (POE) of various values of a decision variable (DV) during the lifecycle of the building due to the earthquake hazard. It is noted that a DV is typically a system performance measure in the interest of various stakeholders, such as monetary losses, downtime, or casualties. Improving the seismic robustness of the CW system is one important objective of the PBEE framework. To identify the performance levels or damage states of the CWs, FEMA 273 [27] lists the general performance levels of the NCs, i.e., operational, immediate occupancy, life safety, and collapse prevention levels. It became the guidelines in seismic design, evaluation, and testing of new and existing CW systems. However, due to the variation of the structural configuration of the CWs, the actual damage behavior is more specific than that described in the guidelines.

Baird et al. [17] found that not all the damaged CWs being investigated in the 2011 Christchurch earthquake met the 'hazard reduction' level (collapse prevention). To accurately include any cases where there was a high risk of serious injury or fatality from façade damage, the 'high hazard' performance level was recommended instead of the 'hazard reduction' level. Operational level requires the CW system to maintain its function where slight damages are allowed but only architectural measures are necessary to repair. No visible cracks occurred in the glass panels, and support system and anchorages performed as well as pre-earthquake conditions. Immediate occupancy level requires that no damages to the fundamental structural components such as the frame, bolts, embedded structural members, etc. Small and minor cracks are acceptable in the CW panels, and the subsequent aesthetic effect is disturbed but the occupants can work in the building safely. Life safety level allows obvious damage to the CW components such as the panels, or the permanent deformation of the structural silicon stick, frame, spider arms, etc., but the integrity of the whole system remains acceptable where falling out of the panels or support system can be prevented. The damages are costly in terms of monetary value or downtime, occupants should be dislodged, and pedestrians should keep a certain distance from the building. High hazard level implies high probability of extensive damage to the CW, breakage of the panels or even collapse of the system where complete retrofit is the only option to claim its function back.

It is worth mentioning that the performance levels of the CWs should involve the main structure to which the CWs are attached. FEMA 389 [119] provides a crossed performance levels for the main structure and the nonstructural system. The flexibility of determining the performance level of the CWs are left to the owners regarding the issues of cost effect, safety insurance, etc. Most recently, FEMA P-58-1 [12] addressed an up-to-date performance-based seismic design procedures for the buildings with NCs, which is helpful to the seismic design and evaluation of the CWs.

5.2. Fragility analysis

5.2.1. Nonstructural systems

Fragility functions provide the probability of exceeding different limit states (such as physical damage, e.g. minor, moderate, extensive, or collapse or even injury levels) given a level of ground shaking. Fragility curves constitute one of the key elements of seismic risk assessment and PBEE. The level of shaking can be quantified using different EDPs, including peak ground acceleration [110], velocity [22], or displacement (or drift ratio) [55], and spectral acceleration [42], velocity, or displacement. Fragility curves are cumulative distribution functions of the structural capacity with respect to a specific limit state, usually corresponding to a physical damage state for the structural system under consideration [89]. They are often described by a lognormal probability distribution function [110]:

$$P(DM \geq dm|EDP = x) = \Phi\left(\frac{\ln(x/x_m)}{\beta}\right) \tag{13}$$

where, $P[DM \geq dm \mid EDP = x]$ denotes the probability that a component will reach or exceed some particular damage state, dm, given that the component was exposed to an EDP whose value is x. On the right hand side of Eq. (13), Φ denotes the cumulative standard normal (Gaussian) distribution function – an S-shaped curve whose first derivative is a familiar bell-shaped curve. The terms x_m and β are parameters of the distribution, which determine its shape.

There are generally four approaches to establish the fragility functions [120], i.e., empirical, judgmental or expert elicitation, analytical and hybrid. Empirical methods are based on post-earthquake surveys and observations of actual damage [8]. They are specific to particular sites and seismotectonic, geological and geotechnical conditions, as well as the properties of the damaged structures or NCs. Expert judgment fragility curves are based on expert opinion and experience [105,9]. Therefore, they are versatile and relatively fast to establish without being affected by the lack of extensive damage data (empirical approaches) or the model of the NCs used in analytical developments. The potential bias in the curves can be reduced by extending the number of experts and by assigning appropriate weight to their estimations, based on their level of expertise [113]. Analytical fragility

curves adopt damage distributions simulated from the analyses of structural (or nonstructural) models under increasing earthquake loads [104,12]. In general, they result in a reduced bias and increased reliability of the vulnerability estimates for different structures compared to expert opinion and thus they are becoming more attractive in terms of the ease and efficiency by which data can be generated. Hybrid methods combine any of the above-mentioned techniques in order to compensate for their respective drawbacks [129,75].

Significant studies have been focused on the construction of fragility curves of building or bridge structures [113,24,55,87], while relatively limited studies on fragility curves of NCs. For restrained and unrestrained block-type NCs, Garcia and Soong [53,54] proposed fragility curves to evaluate their excessive relative displacement and acceleration failure. Hutchinson and Chaudhuri [66] developed fragility curves for the sliding-dominated laboratory equipment and contents where the peak horizontal floor acceleration is the EDP. The inherent uncertainty in the frictional behavior of the unrestrained bench-mounted equipment defined by the static and kinetic coefficients of friction was considered to construct the fragility curves [37]. Badillo-Almaraz et al. [15] developed fragility curves as functions of the spectral accelerations observed in the full-scale tests of a ceiling system. Experimental study in [133] showed that the displacement of the ceiling-perimeter joints governs the cyclic behavior, thus joint displacement is the EDP considered in these fragility curves.

To transform the PEER's PBEE methodology into an applicable professional practice, Porter et al. [113] developed a fragility function to calculate the probability of damage to facility components given the force, deformation, or other EDPs. A list of methods for six situations was intended to assist practitioners to create fragility functions. Generally, there are five steps to generate fragility curves [113]: 1) acquire damage data from analytical, experimental studies, or expert judgement, 2) define the damage states for each performance level, 3) identify EDPs such as acceleration, displacement, velocity, etc., 4) create fragility functions, and 5) assess the quality of the fragility function. With this approach, fragility functions of the hydraulic elevators [110] and traction elevators [111] were developed in terms of peak ground acceleration and peak roof acceleration. The average-conditional fragility functions of mechanical, electrical, and plumbing equipment were developed in terms of floor acceleration [112].

5.2.2. Building CW

Relatively few studies in literature develop the fragility curves for the building CW. Based on the previous experimental tests, Hunt and Stojadinovic [63] presented the damage states of the precast cladding system with fragility curves. Two damage states for the caulking were shown in terms of IDR. As for the window glazing system, four damage states were defined. For the drift-sensitive caulking and window system, the damage states were refined into five categories. Baird [16] developed fragility curves for the threaded rod connections, slotted connections, and panels of the precast reinforced concrete cladding. Sassun [123] defined damage states of the sealant bonded framed window, i.e., the loss of the window sealant bond (Operational level), glass frame contact (cracking initiation, Immediate Occupancy level), and the failure of the glass panel (possible fallout of the glass panel, Life Safety level). These damage states definitions are slightly different from O'Brien et al. [107]. Eva and Hutchinson [50] conducted IP seismic testing of a total of 53 storefront window systems and the experimental damage to the window was categorized into two main groups: 1) three serviceability damage states (SDS), which result in the inability to immediately continue normal service, and 2) two ultimate damage states (UDS), which pose an immediate safety hazard and are not repairable. The SDS identified gasket damage (SDS-1, Operational level), minor glass cracking (SDS-2, Immediate Occupancy level), and detachment of wet glazed attachment system (SDS-3, Immediate Occupancy level). The UDS identified glass cracking (UDS-1, Life Safety level) and glass fallout (UDS-2, Life Safety level, close to High Hazard level). The corresponding magnitudes of the IDRs were provided as well.

With Method B introduced in [107], O'Brien et al. [113] developed fragility curves for a diverse set of mid-rise glass CW and storefront with various configurations. The dispersion parameter β is a measure of the uncertainties in the actual value of demand D (e.g., IDR) a building may experience for the damage state to take place. For cases where a fragility function is generated from a limited experimental database, β is determined as:

$$\beta = \sqrt{\beta_r^2 + \beta_u^2} \tag{14}$$

where β_r is the random variability in the experimental data, β_u is a qualification of the differences between the physical construction details and loading conditions on an actual building as compared to the conditions existing in a laboratory test specimen. The damage states of the CW are: 1) onset of glass cracking corresponding to the Immediate Occupancy level, 2) glass fallout corresponding to the Life Safety level, and 3) gasket seal degradation corresponding to the Immediate Occupancy level. Based on procedures in [107], the fragility curves of the mid-rise and storefront CWs are obtained by the authors of this paper and shown in Figs. 15 and 16. It is obvious that the failure probability of the storefront glass is lower than the mid-rise glass CW system as a result of the magnitude of the glass to frame clearance (GFC).

More comprehensive and applicable fragility curves are necessary to define the damage states and POE of the various CW types, such as point supported CWs, dry-glazed stone cladding, metal CWs, etc. The corresponding method of usage of these curves should be developed as well.

6. Conclusions and future challenges

Historical earthquake damages to the CW systems demonstrated their seismic vulnerability. To understand the seismic design and experimental approaches of CW systems, widely used code provisions and current research developments are reviewed. Some conclusions are listed as follows:

1) The seismic demand of the CW system consists of acceleration and drift demands. Current code provisions proposed the equivalent static force calculation to define the magnitude of the inertia force generated by the floor motions. Relevant factors, e.g. FAA, CAA, CI, and CRM represent the peak floor acceleration amplification effect, component amplification effect, importance level, and dynamic interaction effect between the NCs and the main structure. Their applications to the CW system need further studies. Drift demand is

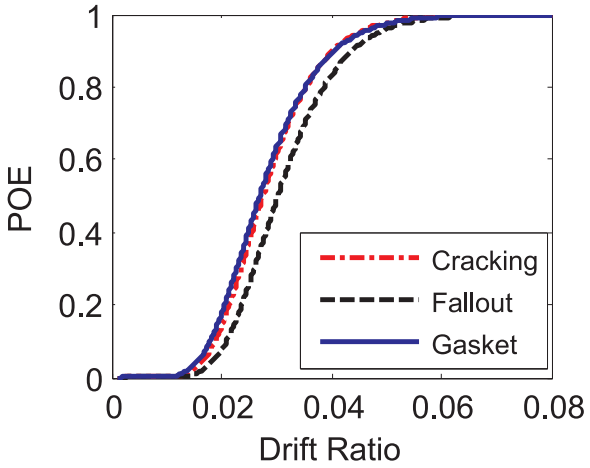

Fig. 15. Fragility curves of mid-rise CW (GFC = 11 mm).

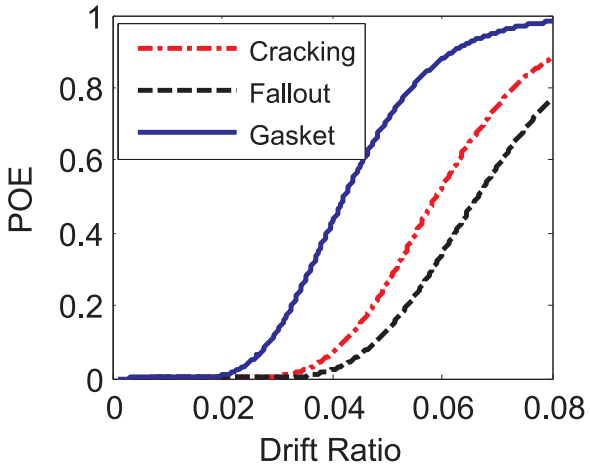

Fig. 16. Fragility curves of storefront (GFC = 15 mm).

represented by the IDR, and is related to the dynamic interstory response of the main structure. Codified IDR demand is helpful to define the deformation ability of the CW system on a specific structure, but comprehensive drift analysis is necessary under the effect of selected ground motions applied to tall or special buildings with complicated configurations. The IP drift capacity of the CW is determined by the silicon stick, gasket, and clear gap between the panel and the frame. More specific experimental studies are necessary to acquire the benchmark IP load-displacement curve, which is useful to understand the interaction of the CW system and the primary structure.

2) Most seismic experimental protocols and studies focused on the IP deformation capacity of the CW system. Simplified static testing protocols provided by AAMA [2], FEMA 461 (2007), and UB-NCs [117], were developed from dynamic analysis of simple structures or closed-form solution of the simplified numerical model. They can be applied to evaluate the IP seismic performance of the CW systems if there are not enough known structural details of the main structure. Shaking table testing is a full dynamic approach, but the test setup needs to be designed carefully to investigate the OP and IP loading behavior in the actual earthquakes.
3) PBEE philosophy and its implementation to the seismic design of CW systems were studied by several researchers. The damage states definition and fragility analysis give the researchers and engineers more options to describe the performance probabilistically.
4) Since earthquake damage to the CW system attracts increasing attention of the society, guaranteeing its seismic safety is important. The FAA factor should be analyzed through comprehensive studies of the buildings with various structural configurations, heights, and site conditions. The CAA factor has to be defined by studying the OP dynamic amplification effect of CWs, such as glass, stone, and metal panels. CRM factor mostly depends on the connection between the CW system and the main structure. Thus, the dynamic properties of the two systems should be understood before determining the applicable factors for different connections. Simplified calculation method should be developed to determine the EDPs for reliable determination of the equivalent static force and for subsequent seismic design approach to assume the seismic safety of the CW system.
5) For the simplified static or the full dynamic testing of the CW, qualified testing protocols should be developed. Floor response analysis of the main structure is necessary to define the characteristics of the floor motion and representative floor spectrum through time history analysis of this floor motion. Representative floor motions compatible to the target floor spectrum should be generated for the dynamic testing of the CW. The relevant technical details such as the time duration, number of peak accelerations, energy content, frequency contents, etc. should be resolved to assure that the generated artificial motions are qualified to evaluate the seismic fragility of the CW. The equivalent static test protocol would thus be developed with reasonable simplifications.
6) There are two critical problems in seismic testing and analysis of the CW system. First, the coupled OP and IP actions of the CW system is hard to be simulate in numerical modeling and in dynamic testing setup. Second, the main structure and CW are hard to model in the laboratory and computational platform. Hybrid simulation is an ideal alterative [48] where the main structure can be simulated computationally, while the physical specimen can be constructed physically in the laboratory. An algorithm defines the relationship between the physical specimen and computational models of the other CWs and structural system. The coupled IP and OP action can be provided by two actuators, the commands to the actuators are updated by the calculated results based on the observed responses of the physical specimen. Slow or real-time hybrid simulations are possible due to available advanced control methods and powerful computational platforms [57].

Acknowledgements

This work was supported by China National Science Foundation with grants number 51608381, 51578405, 51078290, and China National Science and Technology Major Project with grants number 2016YFE0105600, 2013ZX06005004-002-001, and International Joint Research Laboratory of Earthquake Engineering (ILEE) with grant number ILEE-IJRP-P2-P3-2017. The first and fourth authors recognize the additional funding from the Republic of Singapore's National Research Foundation through a grant to the Berkeley Education Alliance for Research in Singapore (BEARS) for Singapore-Berkeley Building Efficiency and Sustainability in the Tropics (SinBerBEST) Program. BEARS has been established by the University of California, Berkeley as a center for intellectual excellence in research and education in Singapore. The authors thank Dr. Selim Günay of UC-Berkeley for his valuable comments on the paper.

References

[1] Akkar S, Yazgan U, Gulkan P. Drift estimates in frame buildings subjected to near-fault ground motions. J Struct Eng 2005;131(7):1014–24.
[2] American Architectural Manufacture Association (AAMA). Recommended dynamic test method for determining the seismic drift causing glass fallout from a wall system, AAMA 501.6-09, Schaumburg, IL; 2009a.
[3] American Architectural Manufacture Association (AAMA). Recommended Static Testing Method for Evaluating Curtain Wall and Storefront Systems Subjected to Seismic and Wind Induced Interstory Drift, AAMA 501.4-09, Schaumburg, IL; 2009b.
[4] American Society of Civil Engineers (ASCE). Minimum Design Loads for Buildings and Other Structures, ASCE 7-95, New York; 1995.
[5] American Society of Civil Engineers (ASCE). Minimum Design Loads for Buildings and Other Structures, SEI/ASCE 7-10, Reston, VA; 2010.
[6] American Society of Civil Engineers (ASCE). Minimum design loads for buildings and other structures, ASCE 7-05, New York; 2006.
[7] American Society of Testing Materials (ASTM). Standard practices for cycle counting in fatigue analysis (E1049-85, reapproved 2011). West Conshohocken, PA: ASTM International; 2011.
[8] Anagnos T. Development of an electrical substation equipment performance database for evaluation of equipment fragilities. PG & E/PEER report. San Jose, CA: Department of Civil and Environmental Engineering, San Jose State University; 1999.
[9] Applied Technology Council, ATC. Earthquake damage evaluation data for California. Report No. ATC-13, Applied Technology Council, Redwood City, CA; 1985.
[10] Applied Technology Council (ATC). Interim protocols for determining seismic performance characteristics of structural and nonstructural components, FEMA 461. Washington, DC: Federal Emergency Management Agency; 2006.
[11] Applied Technology Council (ATC). Interim protocols for seismic performance testing of architectural, mechanical and electrical components (Third draft), ATC-58, Mid-America Center for Earthquake Engineering Research, Multidisciplinary Center for Earthquake Engineering Research. Pacific Earthquake Engineering Research Center; 2005.
[12] Applied Technology Council (ATC). Seismic performance assessment of buildings volume 1 – methodology, FEMA P-58-1. Washington, DC: Federal Emergency

Management Agency; 2012.
[13] Architectural Institute of Japan (AIJ). Design guidelines for earthquake resistant reinforced concrete buildings based on inelastic displacement concept. Tokyo, Japan: Architectural Institute of Japan; 2003.
[14] Bachman RE, Drake RM. Design force provisions for nonstructural elements and model codes, In: Proceedings of the 6th U.S. national conference on earthquake engineering, Earthquake Engineering Research Institute, Seattle, Washington; 1998. p. 12–19.
[15] Badillo-Almaraz H, Whittaker AS, Reinhorn AM. Seismic fragility of suspended ceiling systems. Earthq Spectra 2007;23(1):21–40.
[16] Baird AC. Seismic performance of precast concrete cladding systems[Ph.D thesis]. Christchurch, New Zealand: University of Canterbury; 2014.
[17] Baird A, Palermo A, Pampanin S. Façade damage assessment of concrete buildings in the 2011 Christchurch earthquake. Struct Concr 2012;13(1):3–13.
[18] Behr RA, Belarbi A. Seismic test methods for architectural glazing systems. Earthq Spectra 1996;12(1):129–43.
[19] Behr RA. Seismic performance of architectural glass in mid-rise curtain wall. J Archit Eng 1998;4(3):94–8.
[20] Behr RA, Belarbi A, Brown AT. Seismic performance of architectural glass in a storefront wall system. Earthq Spectra 1995;11(3):367–91.
[21] Behr RA, Belarbi A, Coup JH. Dynamic racking tests of curtain wall glass elements with in-plane and out-of-plane motions. Earthq Eng Struct Dyn 1995;24(1):1–14.
[22] Bilgin H. Generation of fragility curves for typical RC healthcare facilities: emphasis on hospitals in Turkey. J Struct Eng 2016;30(3). [04015056-1-6].
[23] Bouwkamp JG, Meehan JF. Drift limitations imposed by glass, In: Proceedings of the 2nd world conference on earthquake engineering, volume III, Tokyo and Kyoto, Japan,; 1960. p. 1763–78.
[24] Brandenberg SJ, Zhang J, Kashighandi P, Huo Y, Zhao M. Demand fragility surfaces for bridges in liquefied and laterally spreading ground. PEER report No. 2011/01. CA, USA: Pacific Earthquake Engineering Research Center; 2011.
[25] Broker KA, Fisher S, Memari AM. Seismic racking test evaluation of silicon used in a four-sided structural sealant glazed curtain wall system. J ASTM Int 2012;9(3):1–22.
[26] Brueggeman JL, Behr RA, Wulfert H, Memari AM, Kremer PA. Dynamic racking performance of an earthquake isolated curtain wall system. Earthq Spectra 2000;16(4):735–56.
[27] Building Seismic Safety Council (BSSC). NEHRP guidelines for the seismic rehabilitation of buildings, FEMA 273. Washington, DC: Federal Emergency Management Agency; 1997.
[28] Building Seismic Safety Council (BSSC). NEHRP recommended provisions for seismic regulations for new buildings and other structures, Part 1: provisions, FEMA 302. Washington, DC: National Earthquake Hazards Reduction Program; 1997.
[29] Building Seismic Safety Council (BSSC). NEHRP recommended provisions for seismic regulations for new buildings and other structures, Part 2: commentary, FEMA 303. Washington, DC: National Earthquake Hazards Reduction Program; 1997.
[30] Building Seismic Safety Council (BSSC). NEHRP recommended provisions for seismic regulations for new buildings and other structures, Part 1: provisions, FEMA 368. Washington, DC: National Earthquake Hazards Reduction Program; 2000.
[31] Building Seismic Safety Council (BSSC). NEHRP Recommended Provisions for Seismic Regulations for new Buildings and Other structures, Part 1: provisions, FEMA 450. Washington, DC: National Earthquake Hazards Reduction Program; 2003.
[32] Building Seismic Safety Council (BSSC). NEHRP recommended provisions for seismic regulations for new buildings and other structures, FEMA P-750. Washington, DC: National Earthquake Hazards Reduction Program; 2009.
[33] Building Seismic Safety Council (BSSC). NEHRP recommended provisions for the development of seismic regulations for new buildings (and other structures). Washington, DC: National Earthquake Hazards Reduction Program; 1994.
[34] Calvi PM. Relative displacement floor spectra for seismic design of nonstructural elements. J Earthq Eng 2014;18(7):1037–59.
[35] Canadian Standards Association (CSA). Guideline for seismic risk reduction of operational and functional components (OFCs) of buildings, CSA-S832, Rexdale, Ont., Canada; 2006.
[36] Cao Z, Zhang Y, Liu J. Seismic response testing of the glass curtain wall with shaking table, In: Proceedings of the 5th national conference on earthquake engineering, Beijing; 1998. p. 876–71. (in Chinese).
[37] Chaudhuri SR, Hutchinson TC. Fragility of bench-mounted equipment considering uncertain parameters. J Struct Eng 2006;132(6):884–98.
[38] China Academy of Building Research. Curtain wall for building, GB/T 21086-2007. Beijing, China: Standardization Administration of the People's Republic of China; 2007.
[39] China National Standard (CNS). Shaking table test method of earthquake resistant performance for building curtain wall (draft for reviewing), GB/T 18575-201X. China: Administration of Quality Supervision, Inspection and Quarantine of China, Beijing; 2014.
[40] China National Standard (CNS). Shaking table test method of earthquake resistant performance for building curtain wall, GB/T 18575-2001. Beijing, China: Administration of Quality Supervision, Inspection and Quarantine of China; 2001. [in Chinese].
[41] Chopra AK, Chintanapakdee C. Drift spectrum versus modal analysis of structural response to near-fault ground motions. Earthq Spectra 2001;17(2):221–34.
[42] Cimellaro GP, Reinhorn AM, D'Ambrisi A, Stefano MD. Fragility analysis and seismic record selection. J Struct Eng 2011;137(3):379–90.
[43] Coull A, Choudhury JR. Analysis of coupled shear walls. Acids J 1967;64(9):587–93.
[44] Coull A, Choudhury JR. Stresses and deflections in coupled shear walls. Acids J 1967;64(2):65–72.
[45] Courant R, Hilbert D. Methods of mathematical physics. 2. New York: Wiley-VCH; 1989.
[46] Drake RM, Bachman RE. NEHRP provisions for 1994 for nonstructural components. J Archit Eng 1996;2(1):26–31.
[47] Drake RM, Gillengerten JD. Examination of CDMG ground motion data in support of the 1994 NEHRP provisions. In: Proceedings of the 5th U.S. national conference on earthquake engineering, Earthquake Engineering Research Institute, Chicago, Ill; 1994. p. 745–54.
[48] Elkhoraibi T, Mosalam KM. Towards error-free hybrid simulation using mixed variables. Earthq Eng Struct Dyn 2007;36(11):1497–522.
[49] European Committee for Standardization (ECS). Eurocode 8: design of structures for earthquake resistance- Part 1: general rules, seismic actions and rules for buildings, BS EN 1998-1:2004, Brussels; 2005.
[50] Eva C, Hutchinson TC. Experimental evaluation of the in-plane seismic behaviour of storefront window systems. Earthq Spectra 2011;27(4):997–1021.
[51] Fathali S, Lizundia B. Evaluation of ASCE/SEI 7 equations for seismic design of nonstructural components using CSMIP records, In: Proceedings of SMIP12 Seminar on Utilization of Strong Motion Data. Sacramento, CA; 2012.
[52] Federal Emergency Management Agency (FEMA). Quantification of building seismic performance factors, FEMA P695, Washington, DC; 2009.
[53] Garcia DL, Soong TT. Sliding fragility of block-type non-structural components. Part 1: unrestrained components. Earthq Eng Struct Dyn 2003;32(1):111–29.
[54] Garcia DL, Soong TT. Sliding fragility of block-type non-structural components. Part 2: restrained components. Earthq Eng Struct Dyn 2003;32(1):131–49.
[55] Gardoni P, Kiureghian AD, Mosalam KM. Probabilistic capacity models and fragility estimates for reinforced concrete columns based on experimental observations. J Eng Mech 2002;128(10):1024–38.
[56] General Administration of Quality Supervision (GAQS), Inspection and Quarantine of the People's Republic of China. Test method for performance in-plane deformation of curtain wall's, GB/T18250-2000. Beijing, China: China Standards Press; 2001. [in Chinese].
[57] Günay S, Mosalam KM. Enhancement of real-time hybrid simulation on a shaking table configuration with implementation of an advanced control method. Earthq Eng Struct Dyn 2014;44(5):657–75.
[58] Günay S, Mosalam KM. PEER performance-based earthquake engineering methodology, revisited. J Earthq Eng 2013;17(6):829–58.
[59] Gupta A, Krawinkler H. Estimation of seismic drift demands for frame structures. Earthq Eng Struct Dyn 2000;29(9):1287–305.
[60] Gupta A, Krawinkler H. Seismic demands for performance evaluation of steel moment resisting frame structures, John A. Blume Earthquake Engineering Research Center, Report No. 132, Department of Civil Engineering, Stanford University; 1999.
[61] Hall JF (editor). Northridge Earthquake of January 17, 1994, Reconnaissance Report, vol. 1. Earthquake Spectra, Supplement C to vol. 11, Earthquake Engineering research Institute, Oakland, CA; 1995.
[62] Heidebrecht AC, Smith BS. Approximate analysis of tall wall-frame structures. J Struct Eng 1973;99(2):199–221.
[63] Hunt JP, Stojadinovic B. Seismic performance assessment and probabilistic repair cost analysis of precast concrete cladding systems for multistory buildings. PEER report No. 2010/110. Berkeley, CA: Pacific Earthquake Engineering Research Center; 2010.
[64] Huang B, Lu W, Cao W. Discussion on seismic performance indices of architectural curtain walls. China Civil Eng J 2009;42(9):7–12. [in Chinese].
[65] Huang B. Floor seismic demand of the curtain wall system on tall buildings and experimental methodology with shaking table [Ph.D. thesis]. Tongji University; 2014. [in Chinese].
[66] Hutchinson TC, Chaudhuri SR. Simplified expression for seismic fragility estimation of sliding-dominated equipment and contents. Earthq Spectra 2006;22(3):709–32.
[67] Hutchinson TC, Zhang J, Eva C. Development of a drift protocol for seismic performance evaluation considering a damage index concept. Earthq Spectra 2011;27(4):1049–76.
[68] International Code Council (ICC). International building code, International Code Council, Whittier, CA; 2000.
[69] International Code Council (ICC). International building code, International Code Council, Whittier, CA; 2006.
[70] International Code Council (ICC). International building code. International Code Council, Whittier, CA; 2012.
[71] International Code Council Evaluation Service (ICC-ES). Acceptance criteria for seismic qualification by shake-table testing of nonstructural components and systems, AC156, Whittier, CA; 2010.
[72] International Conference of Building Officials (ICBO). Uniform building code. International Conference of Building Officials, Whittier, CA; 1997.
[73] Iwan WD. Drift spectrum: measure on demand for earthquake ground motions. J Struct Eng 1997;123(4):397–404.
[74] Joseph W, Gokhan P, Arash EZ, Ahmad I, Manos M. Floor accelerations in yielding special moment resisting frame structures. Earthq Spectra 2013;29(3):987–1002.
[75] Kappos AJ, Panagopoulos G, Penelis G. A hybrid method for the vulnerability assessment of R/C and URM buildings. Bull Earthq Eng 2006;4(4):391–413.
[76] Karavasilis TL, Bazeos N, Beskos DE. Estimation of seismic drift and ductility demands in planar regular X-braced steel frames. Earthq Eng Struct Dyn 2007;36(15):2273–89.

[77] Kehoe B, Hachem M. Procedures for estimating floor accelerations, Seminar on Seismic Design, Performance, and Retrofit of Nonstructural Components in Critical Facilities, ATC 29–2, Newport Beach, CA; 2003. p. 361–74.
[78] Kim J, Collins KR. Closer look at the drift demand spectrum. J Struct Eng 2002;128(7):942–5.
[79] Krawinkler H, Parisi F, Ibarra L, Ayoub A, Medina R. CUREE-caltech woodframe project publication W-02: development of a testing protocol for wood frame structures. Palo Alto, CA: Consortium of Universities for Research in Earthquake Engineering; 2000.
[80] Kubo T, Hisada Y, Aizawa K, Omiya K, Koizumi S. Investigation of indoor damage and questionable intensity for high-rise building in Tokyo during the great east Japan earthquake. J Jpn Assoc Earthq Eng 2014;14(6):118–41.
[81] Lavelle FM, Bergman LA, Spanos PD. Seismic floor response spectra for a combined system by green's function [NCEER88-0011]. National Center for Earthquake Engineering Research; 1988.
[82] Lin Y, Miranda E. Estimation of maximum roof displacement demands in regular multistory buildings. J Eng Mech 2010;136(1):1–11.
[83] Lu W, Huang B, Cao W. Study on the shaking table test of micro crystal glass curtain wall. Build Struct 2010;40(1):59–61. [in Chinese].
[84] Lu W, Huang B. Study on the shaking table test methods of architectural curtain walls. J Disaster Prev Mitig Eng 2008;28(4):447–53. [in Chinese].
[85] Lu W, Huang B, Chen S, Mosalam KM. Shaking table test method of building curtain walls using floor capacity demand diagrams. Bull Earthq Eng 2016. http://dx.doi.org/10.1007/s10518-016-9866-y.
[86] Lu W, Huang B, Mosalam KM, Chen S. Experimental evaluation of a glass curtain wall of a tall building. Earthq Eng Struct Dyn 2016;45(7):1185–205.
[87] Lupoi G, Franchin P, Lupoi A, Pinto P. Seismic fragility analysis of structural systems. J Eng Mech 2006;132(4):385–95.
[88] Ma C, Yan D. Cyclic loading and shaking table testing of the hidden framed glass curtain wall. Build Struct 1998;3:54–7. [in Chinese].
[89] Mackie K, Stojadinovic B. Fragility curves for reinforced concrete highway overpass bridges. In: Proceedings of the 13th world conference on earthquake engineering, Vancouver, Canada; August 1-6, 2004; 2004.
[90] Medina RA, Krawinkler H. Evaluation of drift demands for the seismic performance assessment of frames. J Struct Eng 2005;131(7):1003–13.
[91] Memari AM, Behr RA, Kremer PA. Dynamic racking crescendo tests on architectural glass fitted with anchored pet film. J Archit Eng 2004;10(1):5–14.
[92] Memari AM, Behr RA, Kremer PA. Seismic behavior of curtain walls containing insulating glass units. J Archit Eng 2003;9(2):70–85.
[93] Memari AM, Kremer PA, Behr RA. Architectural glass panels with rounded corners to mitigate earthquake damage. Earthq Spectra *2006*;22(1):*129*–50.
[94] Memari AM, Kremer PA, Behr RA. Seismic performance of stick-built four-side structural sealant glazing systems and comparison with two-side structural sealant glazing and dry-glazed systems. Adv Civil Eng Mater 2012;1(1):1–22.
[95] Ministry of Housing and Urban-rural of the People's Republic of China (MOHURD). Code for Seismic Design of Buildings, GB 50011-2010. Beijing: China Architecture & Building Press; 2010.
[96] Ministry of Housing and Urban-rural of the People's Republic of China (MOHURD). Technical specification for concrete structures of tall building, JGJ 3-2010. , China: China Architecture & Building Press, Beijing; 2010.
[97] Ministry of Housing and Urban-rural of the People's Republic of China (MOHURD). Technical code for metal and stone wall engineering (draft for reviewing), JGJ102-201X. Beijing, China: China Architecture & Building Press; 2014.
[98] Ministry of Housing and Urban-rural of the People's Republic of China (MOHURD. Technical Code for Glass Curtain Wall Engineering, JGJ102-2003. Beijing, China: China Architecture & Building Press; 2003.
[99] Ministry of Housing and Urban-rural of the People's Republic of China (MOHURD). Technical code for metal and stone curtain walls engineering, JGJ133-2001, China. Beijing, China: Architecture and Building Press; 2001.
[100] Miranda E, Akkar D. Generalized interstory drift spectrum. J Struct Eng 2006;132(6):840–52.
[101] Miranda E, Reyes C. Approximate lateral drift demands in multistory buildings with nonuniform stiffness. J Struct Eng 2002;128(7):840–9.
[102] Miranda E, Taghavi S. Approximate floor acceleration demands in multistory buildings I: formulation. J Struct Eng 2005;131(2):203–11.
[103] Miranda E. Approximate seismic lateral deformation demands in multistory buildings. J Struct Eng 1999;125(4):417–25.
[104] Moehle J, Deierlein G. A framework methodology for performance-based earthquake engineering structure. In: Proceedings of the 13th world conference on earthquake engineering structure, Vancouver, BC, Paper No. 679; 2004.
[105] Mosleh A, Apostolakis G. The assessment of probability distributions from expert opinions with an application to seismic fragility curves. Risk Anal 1986;6(4):447–61.
[106] Mosqueda G, Retamales R, Filiatrault A, Reinhorn A. Testing facility for experimental evaluation of non-structural components under full-scale floor motions. Struct Des Tall Spec Build 2009;18(4):387–404.
[107] O'Brien WC, Memari AM, Kremer PA, Behr RA. Fragility curves for architectural glass in stick-built glazing systems. Earthq Spectra 2012;2(28):639–65.
[108] Pacific Earthquake Engineering Research Center (PEER). PEER NGA Database, retrieved from 〈http://peer.berkeley.edu/nga/〉; 2006.
[109] Pantelides CP, Behr RA. Dynamic in-plane racking tests of curtain wall glass elements. Earthq Eng Struct Dyn 1994;23(2):211–28.
[110] Porter K. Fragility of hydraulic elevators for use in performance-based earthquake engineering. Earthq Spectra 2007;23(2):459–69.
[111] Porter K. Seismic fragility of traction elevators. Earthq Eng Struct Dyn 2016;45(5):819–33.
[112] Porter K, Johnson G, Sheppard R, Bachman R. Fragility of mechanical, electrical, and plumbing equipment. Earthq Spectra 2010;26(2):451–72.
[113] Porter K, Kennedy RK, Bachman R. Creating fragility functions for performance-based earthquake engineering. Earthq Spectra 2007;23(2):471–89.
[114] Priestley MJN, Calvi GM, Kowalsky MJ. Displacement-based seismic design of structures. Pavia, Italy: IUSS Press; 2007.
[115] Chaudhuri SR, Hutchinson TC. Effect of nonlinearity of frame buildings on peak horizontal floor acceleration. J Earthq Eng 2011;15(1):124–42.
[116] Retamales R, Mosqueda G, Filiatrault A, Reinhorn AM. New experimental capabilities and loading protocols for seismic qualification and fragility assessment of nonstructural components, MCEER-08-0026. Buffalo, New York: MCEER, University at Buffalo, State University of New York; 2008.
[117] Retamales R, Mosqueda G, Filiatrault A, Reinhorn AM. Testing protocol for experimental seismic qualification of distributed nonstructural systems. Earthq Spectra 2011;27(3):835–56.
[118] Rodriguez ME, Restrepo JI, Carr AJ. Earthquake-induced floor horizontal accelerations in buildings. Earthq Eng Struct Dyn 2002;31(3):693–718.
[119] Rojahn C. Primer for design professionals: communicating with owners and managers of new buildings on earthquake risk, FEMA 389. Washington, DC: Federal Emergency Management Agency; 2004.
[120] Rossetto T, Elnashai A. Derivation of vulnerability functions for European-type RC structures based on observational data. Eng Struct 2003;25(10):1241–63.
[121] Ruiz-García J, Miranda E. Evaluation of residual drift demands in regular multistorey frames for performance-based seismic assessment. Earthq Eng Struct Dyn 2006;35(13):1609–29.
[122] Sankaranarayanan R. Seismic response of acceleration-sensitive nonstructural components mounted on moment-resisting frame structures [Ph.D. thesis]. University of Maryland; 2007.
[123] Sassun KP. A parametric investigation into the seismic behavior of window glazing systems [Master thesis]. Pavia, Italy: ROSE programme, UME school; 2014.
[124] Shanghai Urban Construction and Communication Commission (SUCCC). Technical code for building curtain wall, DGJ08-56-2012/J12028-2012. Shanghai, China: Shanghai Construction & Construction Material Industry Administration Department; 2012.
[125] Shirazi A. Development of a seismic vulnerability evaluation procedure for architectural curtain walls [Ph.D. thesis]. Pennsylvania State University; 2005.
[126] Shodja AH, Rofooei FR. Using a lumped mass, nonuniform stiffness beam model to obtain the interstory drift spectra. J Struct Eng 2014;140(5):155–64.
[127] Singh MP, Moreschi LM, Suarez LE, Matheu EE. Seismic design forces I: rigid nonstructural components. J Struct Eng 2006;132(10):1524–32.
[128] Singh MP, Moreschi LM, Suarez LE, Matheu EE. Seismic design forces II: flexible nonstructural components. J Struct Eng 2006;132(10):1533–42.
[129] Singhal A, Kiremedjian AS. Bayesian updating of fragilities with application to RC frames. J Struct Eng 1998;124(8):922–9.
[130] Sivanerupan S, Wilson JL, Gad EF, Lam NTK. In-plane drift capacity of contemporary point fixed glass façade systems. J Archit Eng 2014;20(1). [CID: 04013002].
[131] Smith BS, Coull A. Tall building structures: analysis and design. 1st ed New York: Wiley-Interscience; 1991.
[132] Soong TT, Bachman RE, Drake RM. Implications of the 1994 Northridge earthquake on design guidelines for nonstructural components, In: Proceedings of NEHRP conference and workshop on research on the Northridge California Earthquake of January 17, 1994, California Universities for Research in Earthquake Engineering, vol. III; 1998. p. 441–48.
[133] Soroushian S, Maragakis M, Jenkins C. Capacity evaluation of suspended ceiling-perimeter attachments. J Eng Mech 2016;142(2). [04015124-1-14].
[134] Standards New Zealand (NZS). Structural Design Actions, Part 5: Earthquake Actions, NZS 1170.5, Wellington; 2004.
[135] Sucuoglu H, Vallabhan CVG. Behaviour of window glass panels during earthquakes. Eng Struct 1997;19(8):685–94.
[136] Taghavi S, Miranda E. Approximate floor acceleration demands in multistory buildings II: applications. J Struct Eng 2005;131(2):212–20.
[137] Taghavi S. Probabilistic seismic assessment of floor acceleration demands in multistory buildings [Ph.D thesis]. Stanford University; 2006.
[138] Taghavi S, Miranda E. Seismic demand assessment on acceleration-sensitive building nonstructural components, In: Proceedings of the 8th US national conference on earthquake engineering, paper No. 1520, San Francisco, CA; 2006.
[139] The British Standards Institution (BSI). Bases for design of structures - loads, forces and other actions – seismic actions on nonstructural components for building applications, BS ISO 13033:2013. London: BSI standards publication; 2013.
[140] Tongji University (TJU). Code for seismic design of buildings, DGJ08-9-2013. Shanghai: Shanghai Urban Construction and Communication Commission; 2013.
[141] Tongji University (TJU). Technical specification for point supported glass curtain wall, CECS127:2001. Beijing, China: China Association for Engineering Construction Standardization; 2001.
[142] Villaverde R. Approximate procedure for the seismic nonlinear analysis of nonstructural components in buildings. J Seismol Earthq Eng 2005;7(1):9–24.
[143] Villaverde R. Method to improve seismic provisions for nonstructural components in buildings. J Struct Eng 1997;123(4):432–9.
[144] Villaverde R. Simple method to estimate the seismic nonlinear response of nonstructural components in buildings. Eng Struct 2006;28(8):1209–21.
[145] Wang C, Xiao C, Zhao X. Seismic performance test of the curtain wall. Build Struct 2002;32(9):65–7. [in Chinese].
[146] Wang M, Hao R. Shaking table testing of the back-bolt connected stone curtain wall. Build Struct 2001;31(4). [in Chinese].
[147] Wilcoski J, Gambill JB, Smith SJ. The CERL Equipment Fragility and Protection

Procedure (CEFAPP), USACERL Technical report No. 97/58, U.S. Army Corps of Engineers, Champaign, Ill; 1997.

Glossary of abbreviations

CAA: Component acceleration amplification
CI: Component importance
CRM: Component response modification
CW: Curtain wall
DF: Dynamic factor
DV: Decision variable
EDP: Engineering demand parameter
FAA: Floor acceleration amplification
GFC: Glass to frame clearance
IDR: Interstory drift ratio
IP: In-plane
MDOF: Multi-degree of freedom
NC: Nonstructural component
OP: Out-of-plane
PBEE: Performance-based earthquake engineering
PFA: Peak floor acceleration
PGA: Peak ground acceleration
POE: Probability of exceedance
RRS: Required response spectrum
SDOF: Single-degree of freedom
SDS: Serviceability damage states
UDS: Ultimate damage states